

EFFECTS OF HARMATTAN DUST ON VEHICLE AIR FILTERS

By
KNUST

SARSAH EMMANUEL AKONO



A thesis submitted to the School of Graduate Studies, Kwame Nkrumah University of Science and Technology, Kumasi, Ghana, in partial fulfillment of the requirement for the award of the degree of Master of Science in Mechanical Engineering.

February, 2012.

DECLARATION

I hereby declare that this submission is my own research work undertaken at the Department of Mechanical Engineering, Kwame Nkrumah University of Science and Technology, Kumasi, Ghana, towards the MSc degree and that, to the best of my knowledge, it contains no material previously published by another person nor material which has been accepted for the award of any other degree of the University, except where due acknowledgement has been made.

KNUST

Sarsah Emmanuel Akono

Student

Signature

Date

Dr. A. K. SUNNU

Supervisor

Signature

Date

Prof. F.K. FORSON

Head
Department of Mechanical Eng.

Signature

Date

ACKNOWLEDGEMENTS

I wish to express my profound gratitude to my supervisor Dr. A.K. Sunnu for his suggestions, encouragement and patience throughout the entire duration of the project. I am also highly indebted to Prof. F.K. Forson (Head, Mech. Eng. Department, KNUST) for his encouragement. I wish to also thank Prof. Glakpe for his guidance and encouragement, often finding out how I was faring with the thesis work.

I should also mention Mr. Acquah, at the Fluids Mechanics Laboratory, KNUST for his support in helping me get a manometer. I would also like to thank Mr. Adjei of the Civil Engineering Department for his advice on how I could easily collect the dust samples.

I wish to thank Mr. Seth Oduro, the director of NVTI, Kumasi for giving me an engine for my experimental work. My appreciation also goes to Mr. Charles Takyi and all his students at NVTI for their corporation and support in my experimental work. Sincerely, I express my appreciation to my family for their financial support particularly to Mr. Peter Akono Sarsah. In a special way, I recognize the love and patience, as well as the financial support of my fiancée Winnifred Quarthey.

February, 2012.

EMMANUEL AKONO SARSAH

ABSTRACT

Most parts of West Africa experience abnormally high levels of atmospheric dust suspension and deposition from November to March as a result of the dust-laden North-East Trade Winds which blow over the region from the Sahara Desert. This seasonal phenomenon is known as the Harmattan. The Harmattan dust aerosols have different particle characteristics and come in concentrations that are about two to three orders of magnitude higher than the non-Harmattan dust. The performance of engineering devices, systems and equipment therefore needs to be studied during the Harmattan period and the necessary redesign or improvements made.

The behaviour of air filters utilized for removal of dust particles from air during the Harmattan period and the effects they have on the performance of engines in vehicles has been extensively studied. Different aspects of the study were considered including processes of removal of dust particles by filters and the efficiency of the filters in relation to engine performance. Three filters (two paper filters and one foam filter) of different but comparative parameters were used for the study. Inflated dust from untarred road was collected by plastic sheeting materials. Settling Harmattan dust was also collected from the roof top of the College of Engineering new 4-storey classroom and laboratory block.

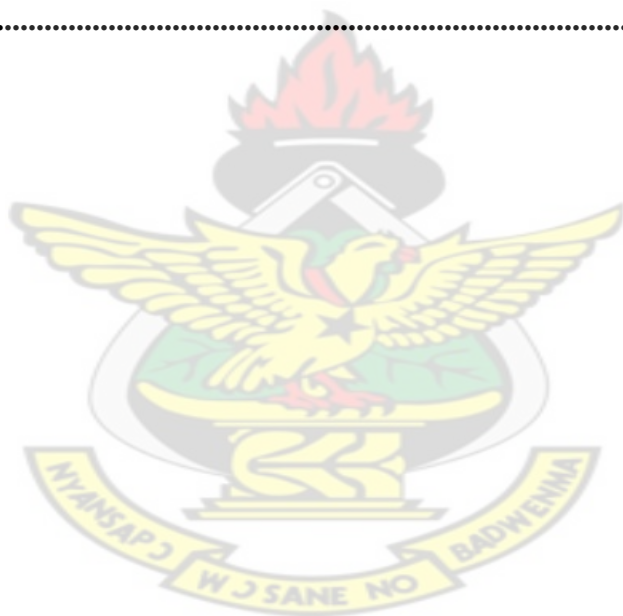
The results of the investigation showed that when the Harmattan season sets in, the pressure drop across filters increase significantly and causes clogging of the filters within a short period (2 to 3 times faster). Air filters in vehicles that ply on untarred roads exhibit higher pressure drops than those used in vehicles on tarred roads. Further steps towards design of these air filters are also discussed.

TABLE OF CONTENTS

DECLARATION	i
ACKNOWLEDGEMENTS	ii
ABSTRACT	iii
ACRONYMS AND ABBREVIATIONS	vii
LIST OF TABLES	viii
LIST OF FIGURES	ix
CHAPTER ONE: INTRODUCTION	1
1.1 Background	1
1.2 Objectives	3
1.3 Justification of the research	3
1.4 Methodology	4
1.5 Structure of Thesis	5
CHAPTER TWO: LITERATURE REVIEW	6
2.1 Principles of Air Filtration	6
2.1.1 Single-Fiber Efficiency	6
2.1.2 Filtration Theory	8
2.1.3 Interception	8
2.1.4 Inertial Impaction.....	9
2.1.5 Brownian Diffusion	11
2.1.6 Gravitational Settling.....	13
2.2 Electrostatic Filtration	14
2.3 Overall Filter Efficiency	15
2.4 Types Of Air Filters Used In Vehicles	15
2.4.1 Paper Filters	15
2.4.2 Foam Filters	16
2.4.3 High Performance Filters	17
2.4.4 Oil Bath Filters.....	18
2.5 Characteristic Structure Of Air Filters	19
2.5.1. Fibrous Filters	19
2.5.2 Porous-membrane Filters	21

2.5.3	Straight-through Pore Membrane Filters	22
2.5.4	Granular-bed Filters	22
2.6	Design Of Air Filters In Vehicles	25
2.6.1	Panel Style	25
2.6.2	Round style	26
2.6.3	Rectangular style:.....	28
2.6.4	Round tapered style.....	29
2.6.5	Conical style.....	30
2.4.1	Benz 200 D	32
2.4.2	Benz 190 D	33
2.4.3	Benz c class 180.....	33
2.4.4	BMW 730.....	34
2.4.5	Hyundai Elantra	35
2.4.6	Hyundai Grace	36
2.4.7	Isuzu KB	36
2.4.7	Mazda 626.....	37
2.4.8	Nissan Maxima	38
2.4.9	Nissan Micera	39
2.4.11	Opel Daewoo Leganza.....	41
2.4.12	Opel Vectra	42
2.4.13	Toyota Coaster	42
2.4.14	Toyota Carina e.....	43
2.4.15	Toyota Corolla LE/CE.....	44
2.4.16	Toyota Tercel.....	44
2.4.17	Toyota Tundra.....	45
2.4.18	Volvo 460.....	46
2.4.19	Volvo S40	46
2.4.20	Volvo S60	47
2.4.21	VW Golf 4.....	48

CHAPTER THREE: EXPERIMENTAL SET-UP AND PROCEDURE.....	49
3.1 Experimental set-up	49
3.2 Experimental procedure	52
CHAPTER FOUR: RESULTS AND DISCUSSION	55
4.1 Results	55
4.2 Discussion	65
CHAPTER FIVE: CONCLUSION AND RECOMMENDATIONS	71
5.1 Conclusion.....	71
5.2 Recommendations	72
REFERENCES.....	74
APPENDIX I	77
APPENDIX II.....	82



ACRONYMS AND ABBREVIATIONS

Rpm	Revolutions per minute
V	Volts
ITCZ	Inter-Tropical Convergence Zone
ΔP	Pressure drop
ECU	Electrical Control Unit
E_ε	Single-fiber efficiency
d_f	Fiber diameter
α	Packing density or solidity
t	Filter thickness
d_p	Particle diameter
K	Kuwabara hydrodynamic factor
C	Cunningham slip correction
U	Air flow velocity
Stk	Stokes number
D	Diffusion coefficient
Pe	Peclet number
k	Boltzmann constant

LIST OF TABLES

Table 2.1 Summary of the salient characteristics of the various types of filters commonly used for aerosol (air) measurement.....	23
Table 3.1 Parameters of filters	53
Table 4.1 (a): Results of experimental measurements for roof top dust (at 0.08 g/s) for filter 1.	55
Table 4.1 (b): Results of experimental measurements for untarred road dust (at 0.14 g/s) for foam filter (1).....	56
Table 4.2 (a): Results of experimental measurements for roof top dust (at 0.08 g/s) for paper filter (2).....	58
Table 4.2 (b): Results of experimental measurements for untarred road dust (at 0.14 g/s) for paper filter (2).....	58
Table 4.3 (a): Results of experimental measurements for roof top dust (at 0.08 g/s) for foam filter (3).	60
Table 4.3 (b): Results of experimental measurements for untarred road dust (at 0.14 g/s) for foam filter (3).....	61

LIST OF FIGURES

Fig. 2.1: Single-fiber efficiency	7
Figure 2.2: Filtration mechanism due to interception	8
Figure 2.3: Filtration mechanism due to impaction	10
Figure 2.4: Filtration mechanism due to diffusion.....	12
Figure 2.5: Principle of electrostatic filtration.....	14
Figure 2.6: A paper filter (source: amazon.com).....	16
Figure 2.7: Foam filter (source: faster-minis.com).....	17
Figure 2.8: Cotton gauze filter (source: amazon.com)	17
Figure 2.9: Abrupt change in direction of air flow	18
Figure 2.10: Principle of operation of an oil bath filter	19
Figure 2.11: Panel style air filter (source: amazon.com).....	25
Figure 2.12: Panel style air filter (source: amazon.com).....	26
Figure 2.13: Round style air filter (source: amazon.com)	27
Figure 2.14: Round style air filter (source: amazon.com)	27
Figure 2.15: Round style air filter (source: amazon.com)	28
Figure 2.16: Rectangular style air filter (source: amazon.com).....	29
Figure 2.17: Round tapered style air filter (source: amazon.com)	30
Figure 2.18: Conical style air filter (source: amazon.com)	31
Figure 2.19: Filtration in Benz 200D.....	32
Figure 2.20: Filtration in Benz 190D.....	33
Figure 2.21: Filtration in Benz c class 180	34
Figure 2.22: Filtration in BMW 730.....	35

Figure 2.24: Filtration in Hyundai Grace.....	36
Figure 2.26: Filtration in Mazda 626	38
Figure 2.27: Filtration in Nissan Maxima.....	39
Figure 2.30: Filtration in Opel Daewoo Leganza.....	41
Figure 2.32: Filtration in Toyota Coaster	43
Figure 2.33: Filtration in Toyota Carina e	43
Figure 2.34: Filtration in Toyota Corolla LE/CE.....	44
Figure 2.35: Filtration in Toyota Tercel.....	45
Figure 2.36: Filtration in Toyota Tundra.....	46
Figure 2.37: Filtration in Volvo 460.....	46
Figure 2.36: Filtration in Volvo S40.....	46
Figure 2.36: Filtration in Volvo S60.....	47
Figure 2.36: Filtration in VW Golf 4.....	48
Fig. 3.1: Experimental set-up.....	51
Figure 4.1(a): Pressure drop across filter 1 for different dust loading rates.	56
Figure 4.1 (b): Air flow across filter 1 for different dust loading rates.	57
Figure 4.1 (c): Engine speed across filter 1 for different dust loading rate.	57
Figure 4.2 (a): Pressure drop across filter 2 for different dust loading rates.	59
Figure 4.2 (b): Air flow across filter 2 for different dust loading rates.	59
Figure 4.2 (c): Engine speed across filter 2 for different dust loading rates.....	60
Figure 4.3 (a): Pressure drop across filter 3 for different dust loading rate.....	61
Figure 4.3 (b): Air flow across filter 3 for different dust loading rate.....	62
Figure 4.3 (c): Engine speed across filter 3 for different dust loading rates.....	62
Figure 4.4 (a): Relation between pressure drop and engine speed for filter 1.	64

Figure 4.4 (b): Relation between pressure drop and engine speed for filter 2..... 65

Figure 4.4 (c): Relation between pressure drop and engine speed for filter 3..... 65

KNUST



CHAPTER ONE

INTRODUCTION

In this chapter, the background, objectives and significance of the research are considered. The chapter discusses the harmattan dust, its impact on vehicle air filters and the overview of air filters.

1.1 Background

The Harmattan is defined as the weather condition in West Africa during the northern winter season, where the atmospheric environment becomes ubiquitously dusty and hazy as a result of the suspension of Saharan dust floating in the northeast winds. Harmattan is the name of the dusty northeast winds that blows in West Africa and by extension the name for the 'season' such as the 'Harmattan season', the 'period' to mean the 'Harmattan period' are used. The Harmattan period lasts for about five months from November to March. Most countries near the Gulf of Guinea in West Africa are affected by this dusty wind phenomenon (Sunnu, 1997).

Meteorologically, the Harmattan affects those areas with latitudes north of the latitudinal position of the Inter-Tropical Convergence Zone (ITCZ), which separates the Saharan dust-laden northeast winds from the southwest monsoon winds. The Harmattan phenomenon is important to governments and scientists because of its effect on ambient air, forest canopy, global circulations, the industry, homes and offices, equipment design and performance, signal transmission, crops and plants, water surfaces, the human body, transportation and horizontal visibility.

In transportation, the Harmattan haze often poses serious hazards in mainly air (for airplanes) and ground (rail and road) transport. Frequent cancellations of flights as a result of poor visibility

cause a heavy loss of revenue annually to the countries affected by the Harmattan episodes. Poor visibility, often caused by thick Saharan dust haze, frequently results in disruption of aviation schedules and sometimes aviation accidents over West Africa sub-region, which can also lead to heavy loss of revenue annually. For example, because of the Saharan dust, visibility was only 300 m at Kano Airport, Nigeria, in the morning of 22 January 1973, when 183 people lost their lives in the crash of a Jordanian airliner (Adedokun et al., 1989).

Air filters are devices attached to the vehicle engine which helps protect the engine from dirt and other debris. Filters are made of a number of materials such as paper, cotton or gauze. Air filters perform important functions to the engine. It filters dirt out of the air entering the engine of the vehicle. Dirt and debris can damage the engine, therefore air filters protect engines. Air filters are like colanders: as the dirt and other damaging debris are picked up by the air, ridges in the filters collect and trap the dirt, preventing it from entering the engine. At the same time, the air is allowed to enter the engine, cleansed of any dirt or debris that might damage the engine. In other words, filters act as a cleansing system that remove any particles or materials that might harm the engine and affect its performance. While air filters do an adequate job of filtering dirt and other particles from entering the engine, they are not 100% effective. This is why, over time, the engine's performance goes down and needs to be repaired or replaced. Air filters do prevent 99% of dirt from passing into the engine (Hinds, pp 99). Still, over a long period of time, dirt and other particles accumulate, clogging and blocking the air filter passages. Once air is blocked from entering the engine, the engine's effectiveness and performance are affected. That is why it is necessary to change air filters once in a while to prevent air blockage.

Air filters are used in applications where air quality is important notably in vehicle engine and cabin, as well as building ventilation systems. Particulate air filters include fibrous materials (pleated-paper filter) which remove solid particulates such as dust from the air and are used in automobile engine air cleaners. The combustion air filter prevents abrasive particulate matter from entering the engine's cylinders, where it would cause mechanical wear. The particulate matter creates friction that can lead to wear and clearance along the walls of the cylinder in the piston-cylinder compartment. This can lead to vibrations being set up.

1.2 Objectives

The main objective of this project is to study the effect of harmattan dust on air filters of road vehicles and the effects they have on the vehicle's engine performance. The study does not include cabin air filters.

1.2.1 Specific Objectives

The specific objectives of this project include;

- To determine the performance characteristics of air filters of vehicles plying tarred and untarred roads.
- To pass a known mass of Harmattan dust over different types of air filters and determine what quantities have been filtered.
- To calculate the filtration efficiency of the different types of the air filters.
- To determine the effect of dust on life of air filters.

1.3 Justification of the research

Information gathered on the field in various transport yards revealed that vehicle routine maintenance is generally scheduled according to the distance travelled by the vehicles. This

means that whether the vehicles are used during the dusty periods or not, maintenance schedules are only carried out based on the distance covered. Studies have also revealed that the Harmattan dust have entirely different particle characteristics (Sunnu, 1997) and come in concentrations that are about two to three orders of magnitude higher than the non-Harmattan dust (Sunnu et al, 2006).

Air filters do prevent 99% of dirt from passing into the engine (Hinds, pp 99). Still, over a long period of time, dirt and other particles accumulate, clogging and blocking the air filter passages. Once air is blocked from entering the engine, the engine's effectiveness and performance are affected.

The significance of this research work is then to determine the engine performance of vehicles as a result of the harmattan dust on air filters and also determine the useful life of the filters.

The project was carried out at the National Vocational and Technical Institute (NVTI) in Kumasi.

1.4 Methodology

The following procedure was used in undertaking this project;

- Examining of different types of engine air filters.
- Setting up an experiment to determine the filtration efficiency of these air filters in relation to engine performance.
- Writing of thesis.

1.5 Structure of Thesis

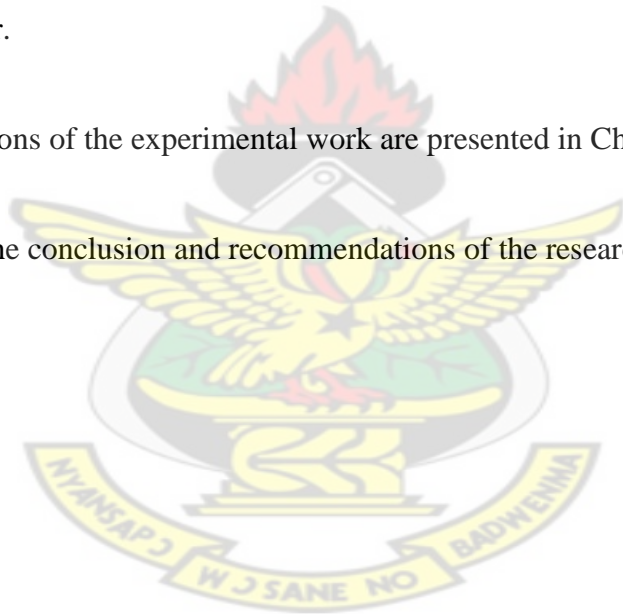
This thesis is organized into five chapters. The introduction, consisting of background, objectives, justification of the study and research methodology, is contained in Chapter One.

Chapter Two contains the literature review of the principles of air filtration, types of air filters in vehicles, design of air filters in vehicles, various materials that are used in the construction of air filters and the review of effects of dust on air filters of vehicles.

Chapter Three presents the description of the experimental set-up. The experimental procedure is also cited in this chapter.

The results and discussions of the experimental work are presented in Chapter Four.

Chapter Five contains the conclusion and recommendations of the research.



CHAPTER TWO

LITERATURE REVIEW

This chapter describes the principles of air filtration, types of air filters in vehicles, different materials used in the construction of vehicle air filters, the characteristics of these materials and the design of air filters in vehicles.

2.1 Principles of Air Filtration

The principles behind how airborne particulates are removed from an air stream by air filters are presented in this section.

2.1.1 Single-Fiber Efficiency

The starting point in characterizing fiber filtration is to consider the capture of particles by a single fiber. The approach is to consider a single fiber, positioned with its axis perpendicular to the air flow in the middle of a filter and analyze the several mechanisms by which particles can be collected on that filter. It is assumed that a particle sticks if it contacts the fiber and is permanently removed from the aerosol stream. The efficiency with which a fiber removes particles from an aerosol stream is defined in terms of a single-fiber efficiency, E_g , a dimensionless particle deposition rate on a unit length of fiber. As shown in Figure 2.1, E_g is the fraction of particles approaching the fiber in the region defined by the projected area of the fiber that are ultimately collected on the fiber.

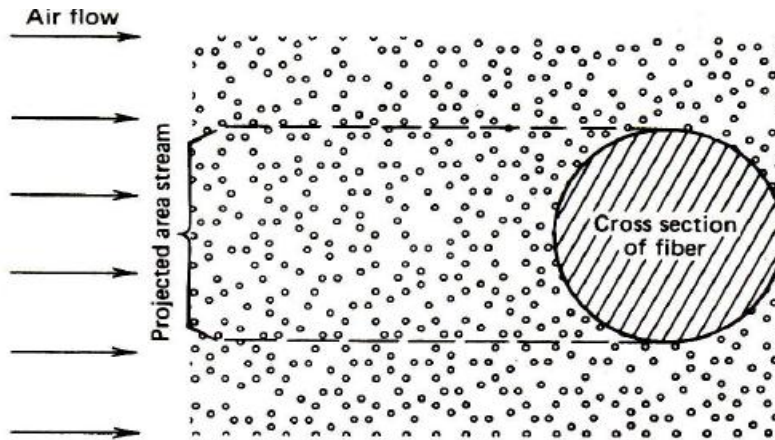


Figure 2.1: Single-fiber efficiency (Hinds, 1999 pp 190)

$$E_{\varepsilon} = \frac{\text{number collected on unit length}}{\text{number geometrically incident on unit length}}$$

Put another way, E_{ε} is the ratio of the number of particles actually collected by a fiber in one second to the number that would have passed through an imaginary outline of the fiber in one second.

The overall efficiency, η of a filter composed of many fibers in a mat can be related to the single fiber efficiency according to Hinds (1999 pp 191) as follows:

$$\eta = 1 - \exp\left[\frac{-4\alpha E_{\varepsilon} t}{\pi d_f}\right]$$

α = packing density or solidity

t = filter thickness

d_f = fiber diameter

2.1.2 Filtration Theory

The removal of airborne particulate (aerosol) from an air stream is called filtration and is accomplished through various means: mechanical and electrostatic means. The mechanical means include interception, inertial impaction, Brownian diffusion and Gravitational settling.

2.1.3 Interception

Collection by interception occurs when a dust particle moves with the airstream and at some point becomes attracted to the media fibers, leaves the airstream and attaches itself to the fibers. This occurs when a dust particle follows a gas streamline that happens to come within one particle radius of the surface of a fiber. Figure 2.2 shows the phenomenon of interception.

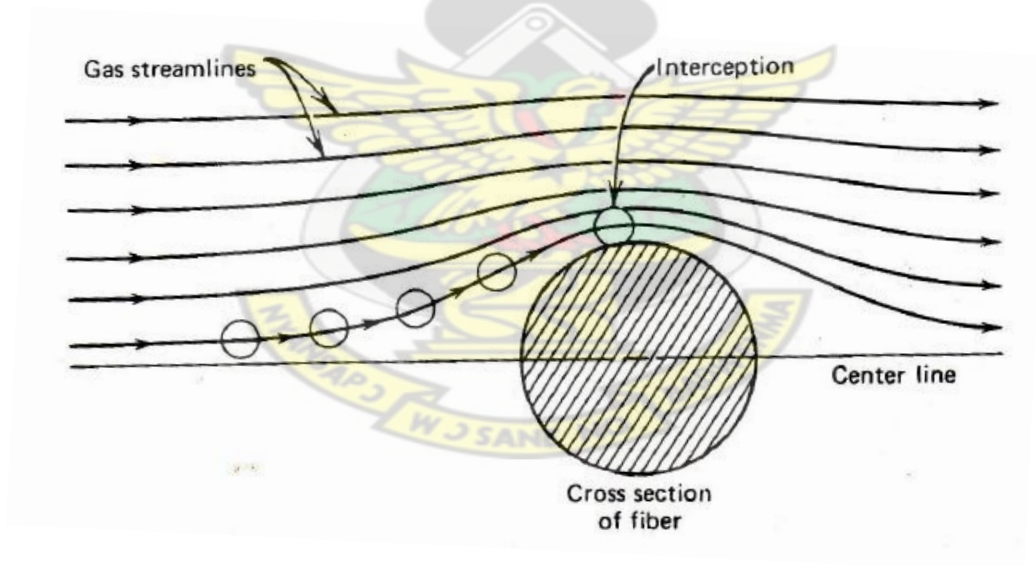


Figure 2.2: Filtration mechanism due to interception (Hinds, 1999 pp 192)

The particle hits the fiber and is captured because of its finite size. Thus, for a given size particle, certain streamlines will result in capture of the particle while other streamlines will not. For pure interception, it is assumed that the dust particles follow the streamlines perfectly, that is, they

have negligible inertia, settling and Brownian motion. Interception is the only mechanism that is not a result of a particle departing from its original gas streamline.

The single-fiber efficiency due to interception depends on the dimensionless parameter, R , according to Hinds (1999 pp 192) where

$$R = \frac{d_p}{d_f}$$

d_p = particlediameter

d_f = fiberdiameter

KNUST

The single-fiber efficiency for interception is given by

$$\eta_{inter} = \frac{1 - \alpha}{K} \frac{R^2}{(1 + R)} \quad (Hinds, 1999)$$

α = packing density or solidity of fiber

K = Kuwabara hydrodynamic factor

2.1.4 Inertial Impaction

Inertial impaction of a dust particle on a fiber occurs when the particle, because of its inertia, is unable to adjust quickly enough to the abruptly changing streamlines near the fiber and crosses those streamlines to hit the fiber and attaches itself. Figure 2.3 shows the inertial impaction mechanism. The streamlines of a fluid around the fiber are curved. Particles with a finite mass and moving with the flow may not follow the streamlines exactly due to their inertia. If the curvature of a streamline is sufficiently large and the mass of a particle is sufficiently high, the particles may deviate far enough from the streamline to collide with the media surface.

Sometimes the air filter media is oiled with a sticky adhesive and therefore operates as a ‘viscous’ filter; the term viscous impingement is therefore used. In order for a particle to impinge onto a target, it must have sufficient kinetic energy to break through the boundary layer surrounding the target. If a particle does not have sufficient kinetic energy, it bounces off the boundary layer back into the general airstream until it encounters another fiber target of the media. In the course of its path through the depth of the filter media the particle will make literally hundreds of attempts at breaking through boundary layers, but on each occasion, will suffer particle bounce and will eventually exit the filter media on the downstream side of the filter. In this manner it is seen that viscous impingement filters favour the larger dust particles. Also it can be seen that the higher the gas velocity through the filter media, greater is the kinetic energy imparted to the particulate. The force that holds a particle to a fiber target is Van Der Waals force (intermolecular attraction). These forces are weak attractive forces, although in most cases are sufficient to hold smaller particles to the target.

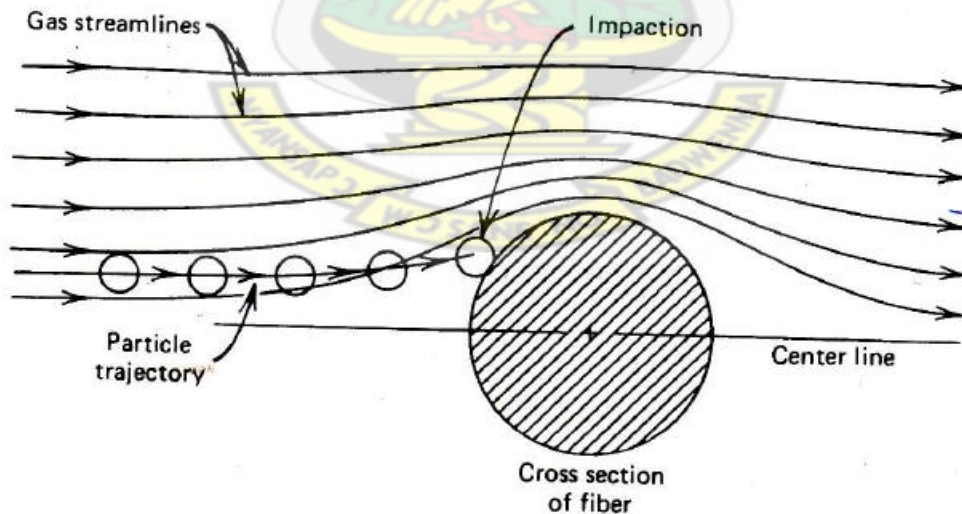


Figure 2.3: Filtration mechanism due to impaction (Hinds, 1999 pp 193)

The inertial impaction mechanism can be studied by the use of the dimensionless Stokes number, defined as (Willeke, 1993 pp 190):

$$Stk = \frac{C d_p^2 \rho_p U}{18 \eta d_f}$$

C = Cunningham slip correction

d_p = particle diameter

ρ_p = density of the particle

U = air flow velocity

η = dynamic viscosity

d_f = fiber diameter

The expression for the filtration efficiency due to inertial impaction is as follows (Willeke, 1993 pp 190):

$$\eta_{imp} = \frac{1}{(2K)^2} [(29.6 - 28 \alpha^{0.62})R^2 - 27.5R^{2.8}]Stk$$

2.1.5 Brownian Diffusion

Brownian motion is the irregular wiggling motion of an aerosol particle in still air caused by random variations in the relentless bombardment of gas molecules against the particle. Diffusion of aerosol particles is the net transport of these particles in a concentration gradient. Filtration by Brownian diffusion occurs when small particles collide with the air molecules and move in an erratic path (Brownian movement). The path allows for the small particle to come in contact with the media and stay attached as shown in Figure 2.4.

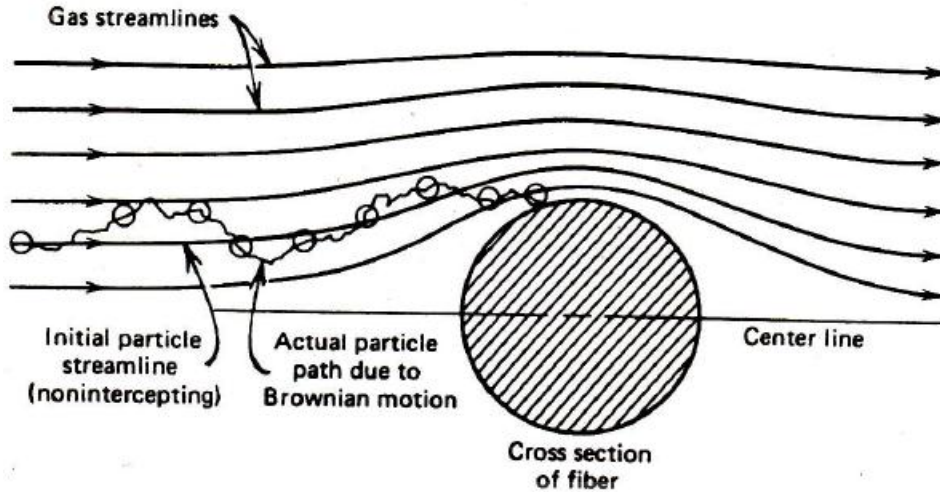


Figure 2.4: Filtration mechanism due to diffusion (Hinds, 1999 pp 194)

The single-fiber efficiency due to diffusion is a function of the dimensionless Peclet number, Pe , defined as (Willeke, 1993 pp 188):

$$Pe = \frac{d_c U}{D}$$

d_c = characteristic length of collecting media

U = the average air velocity inside the filter medium

D = diffusion coefficient of the particle

For pure molecular diffusion, D can be written as according to Willeke (1993 pp 189) as

$$D = \frac{kTC}{3\pi\eta d_p}$$

k = Boltzmann constant

T = absolute temperature

η = air viscosity

d_p = particle diameter

The Cunningham slip correction, C is written as (Willeke, 1993 pp 189):

$$C = 1 + 2.492 \frac{\lambda}{d_p} + 0.84 \frac{\lambda}{d_p} \exp\left(-0.435 \frac{d_p}{\lambda}\right)$$

$\lambda = \text{mean free path of the air molecules}$

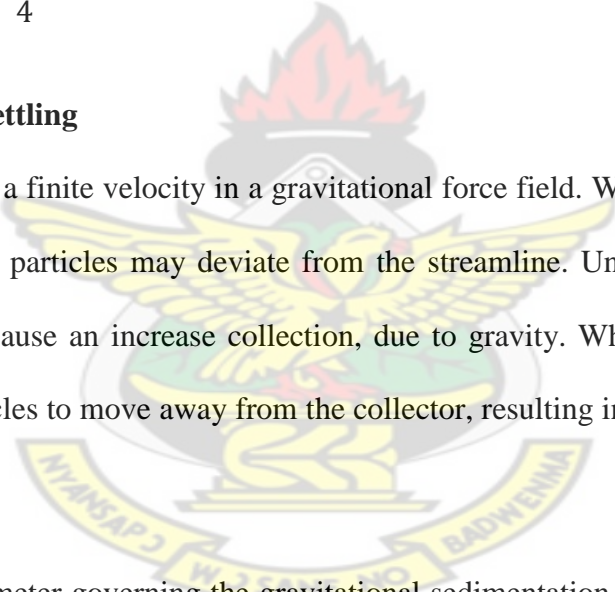
The single-fiber efficiency due to diffusion is given by Willeke (1993, pp 189) as:

$$\eta_{diff} = 2.58 \frac{1 - \alpha}{K} Pe^{-2/3}$$

$K = \text{hydrodynamic factor}$

$$= -\frac{1}{2} \ln \alpha - \frac{3}{4} + \alpha - \frac{\alpha^2}{4}$$

KNUST



2.1.6 Gravitational Settling

Particles will settle with a finite velocity in a gravitational force field. When the settling velocity is sufficiently large, the particles may deviate from the streamline. Under downward filtration conditions, this would cause an increase collection, due to gravity. When flow is upward, this mechanism causes particles to move away from the collector, resulting in a negative contribution to filtration.

The dimensionless parameter governing the gravitational sedimentation mechanism is according to Willeke (1993, pp 190):

$$Gr = \frac{V_g}{U}$$

$U = \text{flow velocity}$

$V_g = \text{settling velocity of particle}$

The single-fiber efficiency due to gravitational settling is given by Willeke (1993, pp 190) as:

$$\eta_{grav} = \frac{Gr}{1 + Gr}$$

2.2 Electrostatic Filtration

Electrostatic filtration is an extremely effective method for removing dust and other small particles from air over a particle size range from about 10 to 0.01 microns (Willeke, pp 192). The principle involved, as shown in Figure 2.5 is that of passing the air through an ionizer screen where electrons colliding with air molecules generate positive ions which adhere to dust and other small particles present, giving them a positive charge. The charged dust particles then enter a region filled with closely spaced parallel metal plates alternatively charged with positive and negative voltages of the order of 6000 volts DC. Positive plates repel the charged particles which are attracted by and retained on the negative plates by electrostatic forces, further supplemented by intermolecular forces, causing the dust to agglomerate.

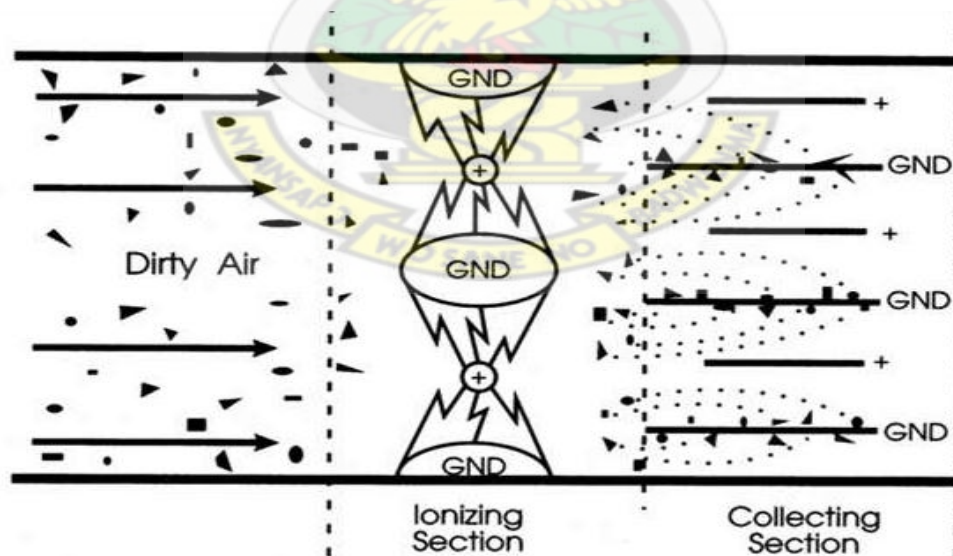


Figure 2.5: Principle of electrostatic filtration (Willeke, pp 192)

2.3 Overall Filter Efficiency

The overall efficiency of a filter can be determined if the total single-fiber efficiency, E_{Σ} is known. The mechanical single-fiber efficiencies are correctly combined as long as each acts independently and is less than 1.0 (Hinds, 1999 pp 196);

$$E_{\Sigma} = \eta_{inter} + \eta_{imp} + \eta_{diff} + \eta_{grav}$$

The overall efficiency of the filter is given by the equation (Hinds, 1999 pp 191):

$$\eta = 1 - \exp\left(\frac{-4\alpha E_{\Sigma} t}{\pi d_f}\right)$$

$t = \text{filter thickness}$

2.4 TYPES OF AIR FILTERS USED IN VEHICLES

The air filter is very important because it helps to keep contaminants such as dust and dirt out of the engine where it could do damage to the vehicle. There are 4 main types of air filters used in cars today. These include paper filters, foam filters, high performance filters and oil bath filters.

2.4.1 Paper Filters

Paper filter elements are the nearly exclusive choice for automobile engine air cleaners, because they are efficient, easy to service and cost-effective. The filter media are considerably different from papers used for writing or packaging. The raw materials are different paper pulps. The pulp may be from softwood, hardwood or fiber crops. For high quality filters, dissolving pulp or mercerized pulp are used. The “paper” in these filters is pleated, as in an accordion fashion, in order to increase surface area. This means that there’s more space for dirt to become trapped. It is widely believed that paper filters flow poorly and thus restrict engine performance. In fact, as

long as a pleated-paper filter is sized appropriately for the airflow volumes encountered in a particular application, such filters present only trivial restriction to flow until the filter has become significantly clogged with dirt. These filters are relatively cheap and easy to replace, but must be done so more frequently than some other filter types. Figure 2.6 shows a paper filter. Particles are captured principally by interception, Brownian motion and inertial impaction mechanisms.

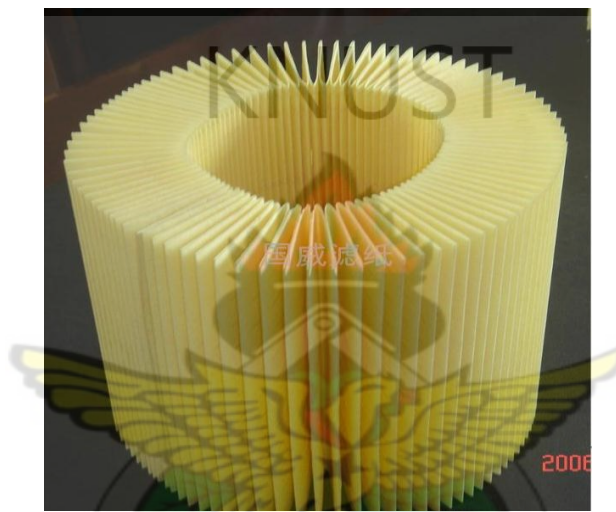


Figure 2.6: A paper filter (Clayton, pp 87)

2.4.2 Foam Filters

Foam filters are very popular for dusty areas and in sports such as off-road and rally racing. This is because the foam is a polyurethane that is soaked in oil. These types of filters come in *different grades* of foam and can vary in *thickness* as well; these factors contribute to the airflow resistance and the dirt capacity. Again, since these can handle such high volumes of dirt, they are very popular in off road motorsports. Particles are captured by Brownian motion and inertial impaction mechanisms. Shown in Figure 2.7 is a foam filter.



Figure 2.7: Foam filter (Clayton, pp 87)

2.4.3 High Performance Filters

High performance filters (they have about 99% filtration efficiency) are typically made of cotton gauze as shown in Figure 2.8 and are more popular among vehicles such as sports cars, road-rally cars, competition trucks or in applications such as increase in air intake and power of the engine. These filters can be a bit pricier than the others, especially if bought with a cold-air intake system. Filtration mechanisms due to impaction and interception are predominant in the capture of particles.



Figure 2.8: Cotton gauze filter (Clayton, pp 90)

2.4.4 Oil Bath Filters

One of the oldest types of air filter is that of the oil bath. This was what was used in vehicles until the introduction of paper filters in the sixties. The general principle of an oil bath air cleaner is that incoming air is sucked downwards through the filter system towards the bowl containing a reservoir of oil as illustrated in Figure 2.9. The airflow has to make an abrupt change in direction from travelling downwards towards the oil pool before heading back upwards to the filter outlet. The air changes direction easily, however any dirt carried in the air is unable to make the turn due to its inertia so it continues straight onto the oil where it is trapped.

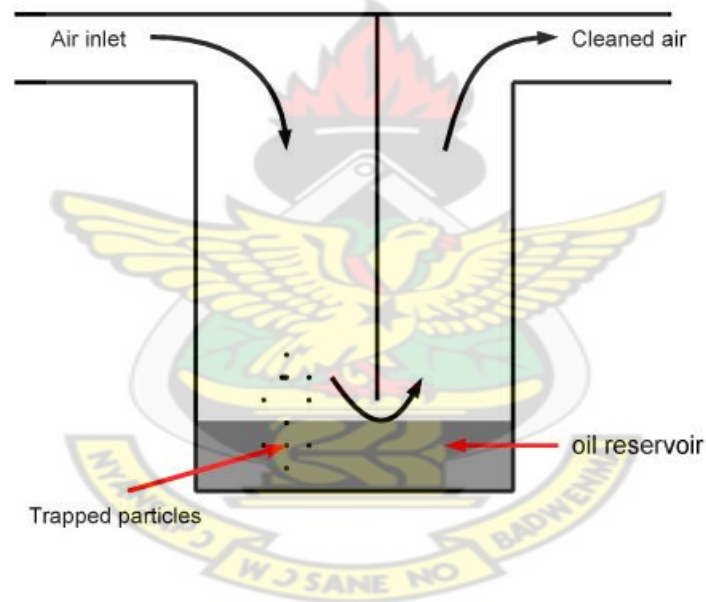


Figure 2.9: Abrupt change in direction of air flow (Heisler, pp 409)

Tractor engines work in dusty conditions and so the majority of manufacturers have progressed this principle to make it even more efficient at capturing the remaining particles of dirt. The bottom of the air inlet pipe is submersed below the oil level so that the air must pass through the oil (See Figure. 2.10). As the air heads back upwards under suction through the filter it now must pass through a packing material (fiber, mesh, foam or metal shavings). The air carries with it

some oil up into the packing material where smaller dust particles become trapped and the cleaned air continues upwards and out of the air cleaner. The process of the air carrying oil with it up into the packing material has the effect of washing the dirt particles back down into the reservoir

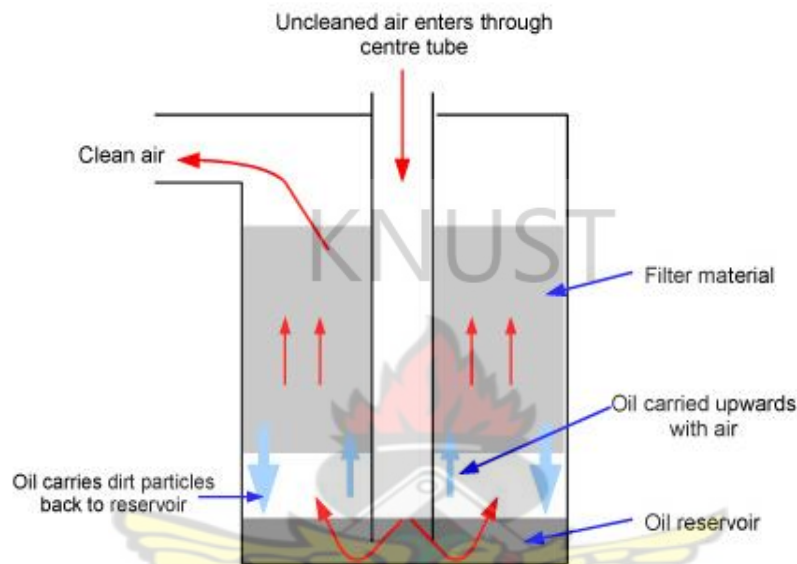


Figure 2.10: Principle of operation of an oil bath filter (Heisler, pp 409)

2.5 CHARACTERISTIC STRUCTURE OF AIR FILTERS

A logical way to classify air filters is to divide them by their characteristic structure. In general, filters used for air sampling may be classified as fibrous filters, porous-membrane filters, straight-through membrane filters and granular-bed filters, according to their structure.

2.5.1. Fibrous Filters

Fibrous filters consist of a mat of individual fibers. Generally, filter porosity (porosity refers to the ratio of open space in a filter matrix to the amount of volume taken by the filter media itself) is relatively high ranging from about 0.6 to 0.999 (Hinds, 1999). Porosities of less than 0.6 are not typically found in fibrous filters because of the difficulties in effectively compressing the

component fibers into a smaller thin layer. Typically, a filter with high porosity will have a more open structure and therefore, higher flow with lower pressure drops. High porosity does not necessarily mean that the filter will remove particles better than a low porosity filter.

Fiber sizes range from less than 1 μm to several hundred micrometers (Hinds, 1999). The range of fiber diameters for a given filter is usually very diverse, although some types of fibrous filters may consist of fibers of a uniform size. Often, the filters are fabricated using a binder material to hold individual fibers together. The mass for the binder material can be as high as 10% of the filter material (Hinds, 1999). Binder-free filters are generally selected for aerosol measurement because of the interferences caused by the presence of the organic binder in the filter. The materials used for fibrous filters include cellulose, glass, quartz and plastic fibers. Sometimes, mixed fibers of cellulose, asbestos and glass are also used as filters for certain low-cost qualitative sampling applications.

Cellulose fiber (paper) filters were used once very widely for general-purpose air sampling. The filters are inexpensive, come in various sizes and have good mechanical strength and low pressure drop characteristics. Some of the critical limitations of cellulose fiber filters are their moisture sensitivity and relatively low filtration efficiency for sub-micrometer particles.

Glass fiber filters typically have a higher pressure drop than paper filters and often provide filtration efficiencies of greater than 99% for particles larger than 0.3 μm (Hinds, 1999). The filters are more expensive than paper filters. However, glass fiber filters are less affected by moisture than cellulose fiber filters. Glass fiber filters are widely used as the standard filter media for high-volume air sampling. Teflon-coated glass fiber filters overcome some of the

inherent inadequacies of glass fiber filters by being inert to catalyzing chemical transformations as well as by being less moisture-sensitive.

Quartz fiber filters are commonly used in high-volume air sampling applications involving subsequent chemical analyses such as atomic absorption, due to their low trace contamination levels, as well as their relative inertness and ability to be baked at high temperatures to remove trace organic contaminants.

Polystyrene fiber filters have been used for sampling purposes to a limited extent. These filters have poorer mechanical strength than cellulose filters. However, their filtration efficiency is comparable to that of glass fiber filters. Other plastic materials used in filters include polyvinyl chloride and Dacron. For special applications involving high temperatures and corrosive environments, filters made of stainless steel fibers have also been recently introduced.

2.5.2 Porous-membrane Filters

Membrane filters are gels formed from a colloidal solution and have a very complicated and uniform microstructure providing a tortuous or irregular air flow path. Often, the complex filter structure consists of a series of layers formed by different processes, depending upon the manufacturing technique. The pore sizes provided by manufacturers often do not match any of the physical filter pores or structural characteristics and are defined from liquid filtration. Liquid filtration involves the removal of contaminant particles in a fluid system. The grade of filter chosen for a specific application is usually determined by the size of the particle to be removed. In general, the pressure drop and the particle collection efficiency are very high. Particles are captured by the surfaces provided by the filter structure, principally by Brownian motion and inertial impaction mechanisms.

2.5.3 Straight-through Pore Membrane Filters

These types of filters consist of a polycarbonate membrane with straight-through pores of a uniform size. They are very often called Nuclepore filters after their original manufacturer, Nuclepore Corporation. The filters are manufactured by subjecting polycarbonate membranes to neutron bombardment, followed by an etching process that produces uniform-sized pores in the membrane. The number of pores is controlled by the bombardment time and the pore size is determined by the etching time. Capillary pore membrane filters have a very different and simpler structure compared to porous-membrane filters. They consist of a very smooth and translucent surface with straight-through capillary holes across the membrane structure. Straight-through pore membrane filters are widely used for particle analysis using surface analytical techniques such as light and electron microscopy.

2.5.4 Granular-bed Filters

For specialized applications, aerosol sampling may be performed using a granular-or packed-bed filter. Filtration is accomplished by passing particle-laden air through a bed consisting of granules and recovering aerosols afterwards by extraction procedures. A major advantage of aerosol sampling by granular beds is that by selecting the proper bed media, both particulate and gaseous pollutants can be simultaneously collected. Possibilities for using this method at high temperature and pressure also make this filter type attractive. Granules of activated charcoal, XAD-2, Florisil, Tenax, sugar, naphthalene, glass, sand, quartz and metal beads have been used. XAD-2 and Tenax are polymeric adsorbent resins made of spherical granules and Florisil is a magnesia-silica material. Aerosols are usually recovered from the granular media for chemical analysis by washing, volatilization or the use of solvents.

Table 2.1 Summary of the salient characteristics of the various types of filters commonly used for aerosol (air) measurement

Filter type	Characteristics
Fibrous filters	<ul style="list-style-type: none"> • Mat/weave of fibers with diameters of 0.1 – 100 μm. Cellulose or wood (paper), glass, quartz and polymer fiber filters are available. • Porosities of 60% - 99%, thickness of 0.15 – 0.5 mm. • Particle collection is throughout the depth of the filter from interception, impaction and diffusion onto fibers. • High particle collection efficiencies require low air velocities. • Pressure drops are the lowest among all filter under comparable conditions. • Used in high-volume air sampling applications.
Porous-membrane filters	<ul style="list-style-type: none"> • Microporous membranes with tortuous pores throughout the structure. • Polymer, sintered metal and ceramic microporous filters available. • Pores sizes (determined from liquid filtration) in the range 0.02 – 10 μm. • Porosities of less than 85% and thickness of 0.05 – 0.2 mm. • Particle collection through attachment to microstructure elements. • High collection efficiencies but highest pressure drop among all filters. • Particularly used in liquid filtration.

<p>Straight-through pore filters</p>	<ul style="list-style-type: none"> • Thin polycarbonate films (10 μm) with cylindrical pores perpendicular to film surface, with diameters in the range 0.1 – 8 μm. • Porosities are low, in the range 5% - 10%. • Particle collection through impaction and interception near the pores and diffusion to tube walls of pores. • Collection efficiencies are intermediate between fibrous and microporous membrane. • Pressure drops are significantly higher than fibrous filters and comparable or higher than microporous membrane filters for equivalent collection efficiency. • Are widely used for particle analysis using surface and analytical techniques.
<p>Granular-bed filters</p>	<ul style="list-style-type: none"> • For special sampling, granules of specialty chemicals, sugar, naphthalene, sand, metals, glass beads are used. • Samples are recovered by washing or volatilization. • Granular bead sizes range from 200 μm to a few mm. • Filtration is achieved by impaction, interception, diffusion and gravitation. • Filter porosities of 40%-60% for stationary beds. • Low collection efficiency due to large granule size. To enhance diffusion low flow is used; bed depth is increased or smaller granules are used. • Used in specialized applications.

2.6 DESIGN OF AIR FILTERS IN VEHICLES

Air filters used in vehicles have different designs and are made of different materials of pore sizes up to 100 μm . Some of the different designs that are currently in use in vehicles include panel style, round style, rectangular style, round tapered style and conical style.

2.6.1 Panel Style

These are high performance air filters designed to maximize air flow while trapping harmful dirt particles, resulting in increased horsepower, improved throttle response and better fuel mileage. They are manufactured using two layers of tightly-interwoven material, cross-weaving one fine and one medium layer, creating a fabric that is thinner and stronger, increase horsepower and acceleration. They offer high air flow with excellent filtration. They are washable and reusable.

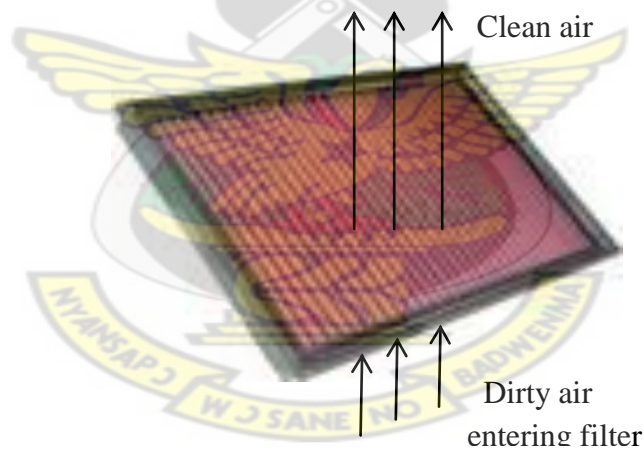


Figure 2.11: Panel style air filter (Clayton, pp 91)

Unclean air passes over the underside of the filter and due to the suction action of the engine the air is drawn from the upper side into the engine. Aerosol particles are then filtered off from the air by the fibers of the filter. Clean air now enters the engine for combustion.

Shown in Figure 2.11 above is a typical high flow air filter, panel style with height 2.9 cm, outside length 35.2 and an outside width of 24.4 cm, used in BMW 524td.

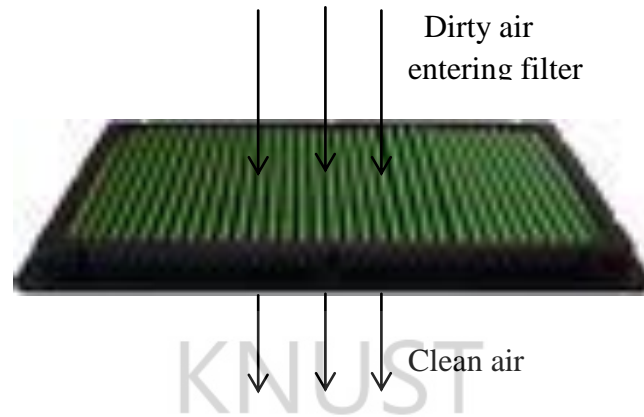


Figure 2.12: Panel style air filter (Clayton, pp 91)

Shown in Figure 2.12 above is the type used in Infiniti 135 model and is made of cotton gauze.

2.6.2 Round style

These air filters have up to 99% filtration efficiency. Most feature permaleat construction that forms divides between pleats and prevents bunching for insured uniform air flow. Most have a radial seal gasket formed from a special urethane compound that will not degrade under temperature extremes and even under changes in restriction or vibration. They also have spiral glue binding for added pleat stability and flexible outer edges that allow deflection for easy insertion and removal.



Figure 2.13: Round style air filter (Clayton, pp 92)

Air carrying airborne particulates flows around the circumference of the filter and due to the suction action of the engine, the air is drawn into from around the periphery of the filter into the cavity. The fibers then filter the dirty air and make it clean before it enters the engine. The same filtration mechanism is used for all round style air filters (See Figure 2.14 and Figure 2.15).

Figure 2.13 shows a typical high flow air filter, round style with height 21.6 cm, internal diameter of 10.2 cm and an outside diameter of 14.6 cm, used in Ferrari Dino 246 GTS and constructed of cotton gauze material.



Figure 2.14: Round style air filter (Clayton, pp 92)

Shown in Figure 2.14 is a round style air filter used in Ford 300 with an outside diameter of 21.4 cm, an internal diameter of 16.7 cm and a length of 8.2 cm. The material used for its construction is paper.

Also shown in Figure 2.15 is another design of Ford 300 air filter that utilizes two integral filtering elements and is constructed of paper. It lasts 50% longer and stops 50% more dirt than any other brand.



Figure 2.15: Round style air filter (Clayton, pp 94)

2.6.3 Rectangular style:

These are high performance air filters designed to maximize air flow while trapping harmful dirt particles, resulting in increased horsepower, improved throttle response and better fuel mileage.



Figure 2.16: Rectangular style air filter (Clayton, pp 95)

Air carrying airborne particulates flows around the circumference of the filter and due to the suction action of the engine, the air is drawn into from around the periphery of the filter into the cavity. The fibers then filter the dirty air and make it clean before it enters the engine.

In Figure 2.16 above is shown a high flow air filter with height 5.7 cm and made of cotton gauze material. The type shown above is used in Ferrari 308 GTS.

2.6.4 Round tapered style

These are high performance washable and reusable filters that last longer, made with ultra-strong molded pliable rubber flanges which absorb vibration, allow secure attachment and can be stretched up to 1/16 to fit in-between sizes.

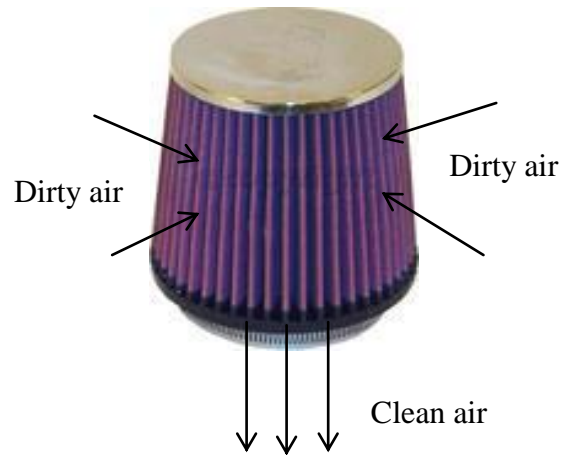


Figure 2.17: Round tapered style air filter (Clayton, pp 96)

Air carrying airborne particulates flows around the circumference of the filter and due to the suction action of the engine, the air is drawn into from around the periphery of the filter into the cavity. The fibers then filter the dirty air and make it clean before it enters the engine. The same principle of operation is used in the conical style air filters (Figure 2.18).

Shown in Figure 2.17 above is a round tapered air filter with outside diameter 13.7 cm, flange length 1.6 cm and flange inside diameter 10.2 cm. It is used in Hyundai Accent model and is made of cotton gauze.

2.6.5 Conical style

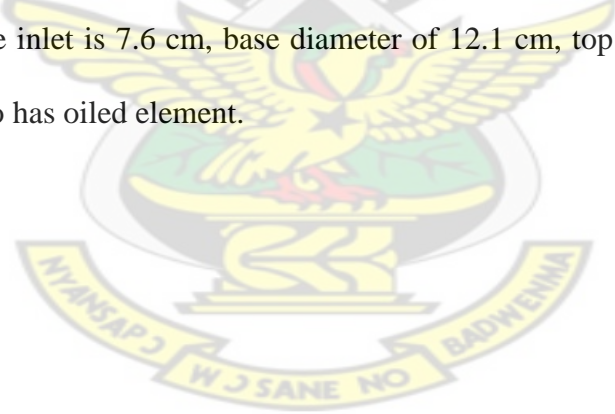
These air filters have up to 99.9% filtration efficiency. They are usually made of the highest quality textiles pleated between the top and bottom aluminium screen. They offer very high air flow rate and longest service life. They are cleanable and reusable and last up to 19312 km before cleaning is required depending on drive conditions.



Figure 2.18: Conical style air filter (Clayton, pp 97)

Air carrying airborne particulates flows around the circumference of the filter and due to the suction action of the engine, the air is drawn into from around the periphery of the filter into the cavity. The fibers then filter the dirty air and make it clean before it enters the engine.

Shown in Figure 2.18 is Volant pro-5 air filter used in Toyota Tacoma model that is made of cotton gauze. The flange inlet is 7.6 cm, base diameter of 12.1 cm, top diameter 12.1 cm and a height of 15.2 cm. It also has oiled element.



2.7 AIR FILTRATION THEORY IN VEHICLES

The various mechanisms and arrangements employed in different vehicles for filtering airborne particulates before the air enters the engine for combustion are presented in this section.

2.4.1 Benz 200 D

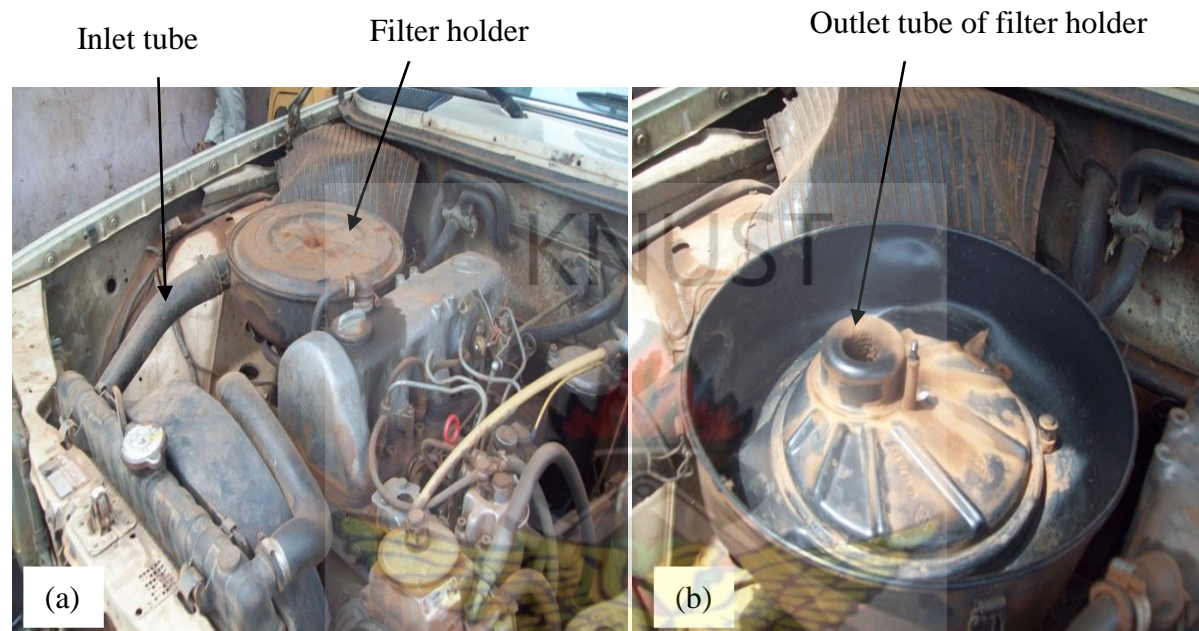


Figure 2.19 (a) Benz 200D filter holder with inlet tube. (b) Inside of filter holder

In this vehicle, the filter holder is located to the left and back of the engine compartment as shown in Figure 2.19 (a). The filter holder is a circular type with a long inlet tube with its opening close to the front of the engine compartment and uses a round filter. Air from the atmosphere is drawn through the inlet and atmospheric aerosol is filtered by the filter. The filtered air is then drawn through the outlet of the holder which is located some distance away to the left of the holder's centre. Figure 2.19 (b) shows the inside of the circular holder used in this vehicle.

2.4.2 Benz 190 D

This is also a diesel engine that uses a panel style filter in its holder. Because of the arrangement of the filter holder as shown in Figure 2.20 (a), the filter has a metal strip placed on top to keep the filter in place (Figure 2.20 b). The filter element is made of paper. The holder is located near the centre of the engine compartment and to the right. Air filtered by the filter before it enters the engine.

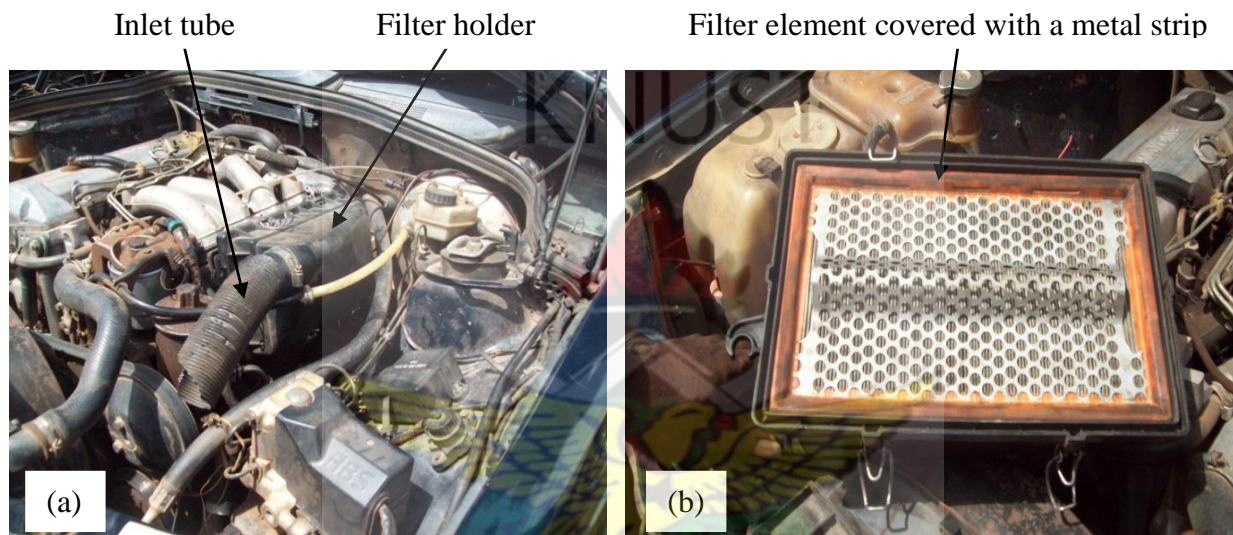


Figure 2.20 (a) Benz 190D filter holder with inlet tube. (b) Filter element of Benz 190 D

2.4.3 Benz c class 180

The filter holder is located to the far left and just at the front of the engine compartment as shown in Figure 2.21 (a). The filter element is a paper type shown in Figure 2.21 (b) and is specially designed to achieve high filtration efficiency as it can filter off more aerosol particles. Since this is a petrol engine type, it has an air flow sensor located just at the entrance of the engine inlet to record the air quantity and communicate it to the engine's ECU.

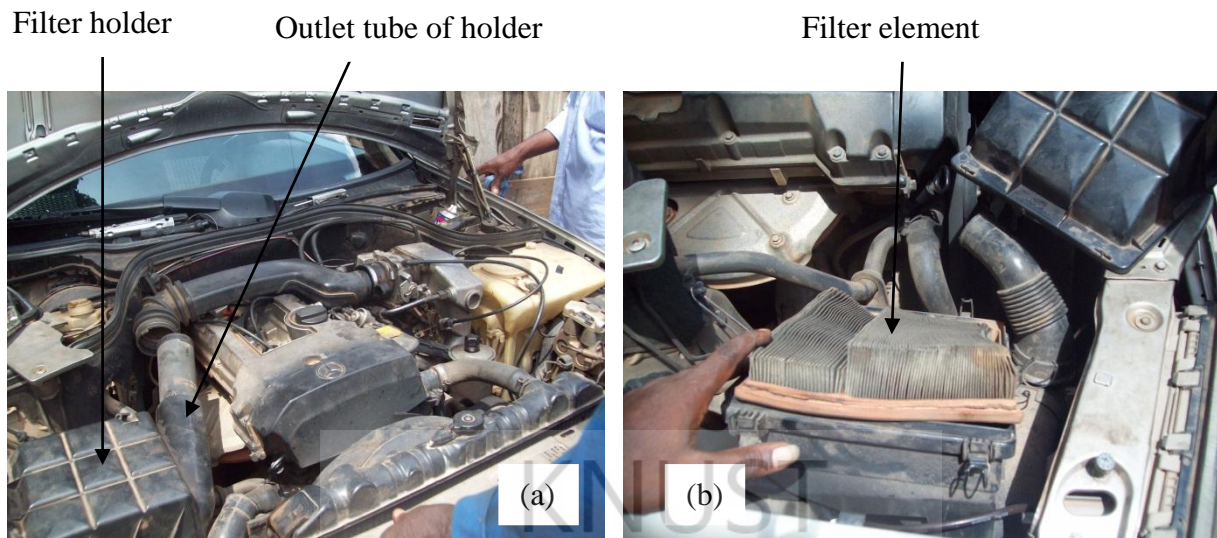


Figure 2.21 (a) Benz c class 180 filter holder. (b) Filter element of Benz c class 180

2.4.4 BMW 730

As shown in Figure 2.22 (a), the filter holder of this petrol engine vehicle is located to the left and at the front of the engine compartment. The inlet tube of the holder is attached directly to the vehicle's front. The filter element is a panel style type made of paper as shown in Figure 2.22 (b). It is also equipped with an air flow sensor.

Air flow sensor

Filter holder

Inlet tube of holder

Filter element

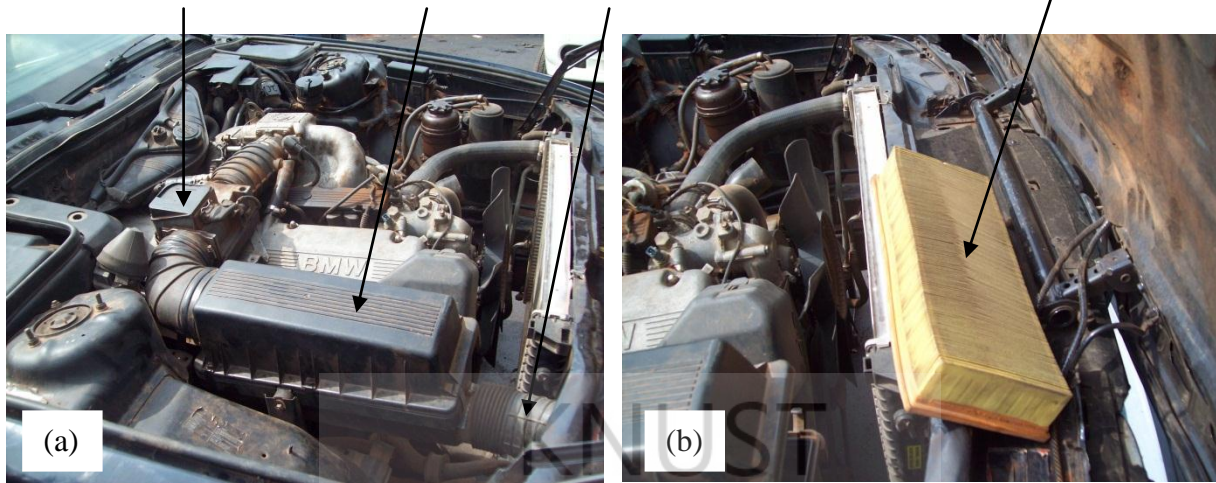


Figure 2.22 (a) BMW 730 filter holder with inlet tube. (b) BMW 730 filter element

2.4.5 Hyundai Elantra

This uses a panel style air filter made of paper specially designed in three layers as shown in Figure 2.23 (b). The holder is placed to the right and back of the engine compartment. The inlet of the holder is a short one with its opening in the engine compartment as shown in Figure 2.23 (a).

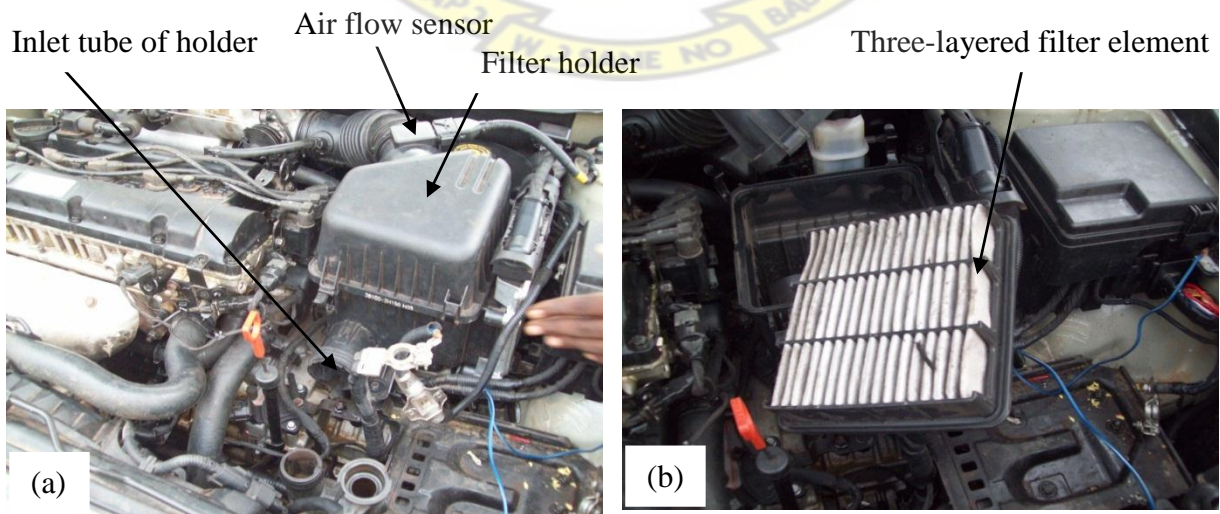


Figure 2.23 (a) Hyundai Elantra filter holder with inlet tube. (b) Hyundai Elantra filter element

2.4.6 Hyundai Grace

A cylindrical filter element is fitted in this vehicle. A metallic element with circular openings covers the element as shown in Figure 2.24 (b). The metal cover blocks some atmospheric aerosols from entering the filter. The openings created allow more air to enter for combustion. The filter element is a paper type. Atmospheric aerosol filtered off settles in a plastic container around the filter element and inside the holder shown in Figure 2.24(a). Air enters the filter element from under the vehicle.

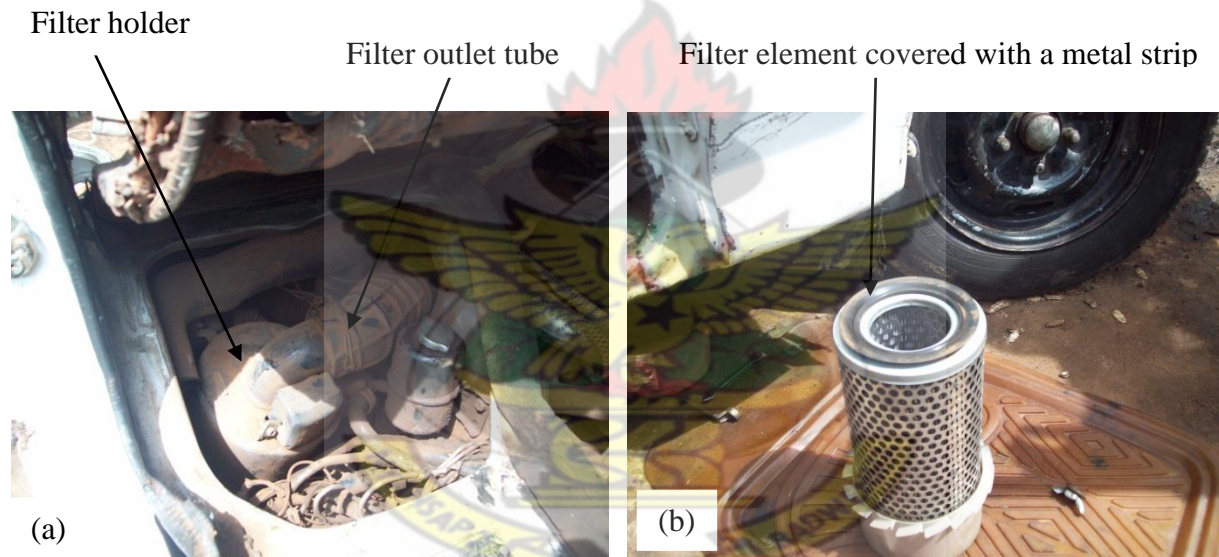


Figure 2.24 (a) Hyundai Grace filter holder. (b) Hyundai Grace filter element

2.4.7 Isuzu KB

The filter element is a cylindrical style with a larger diameter than the Hyundai Grace type. The element is also covered with a metallic element with circular openings halfway the metallic element shown in Figure 2.25 (b). This arrangement prevents more atmospheric aerosol from

entering the filter. The outlet tube of the holder shown in Figure 2.25 (a) is placed on top of the holder to direct the filtered air into the engine.

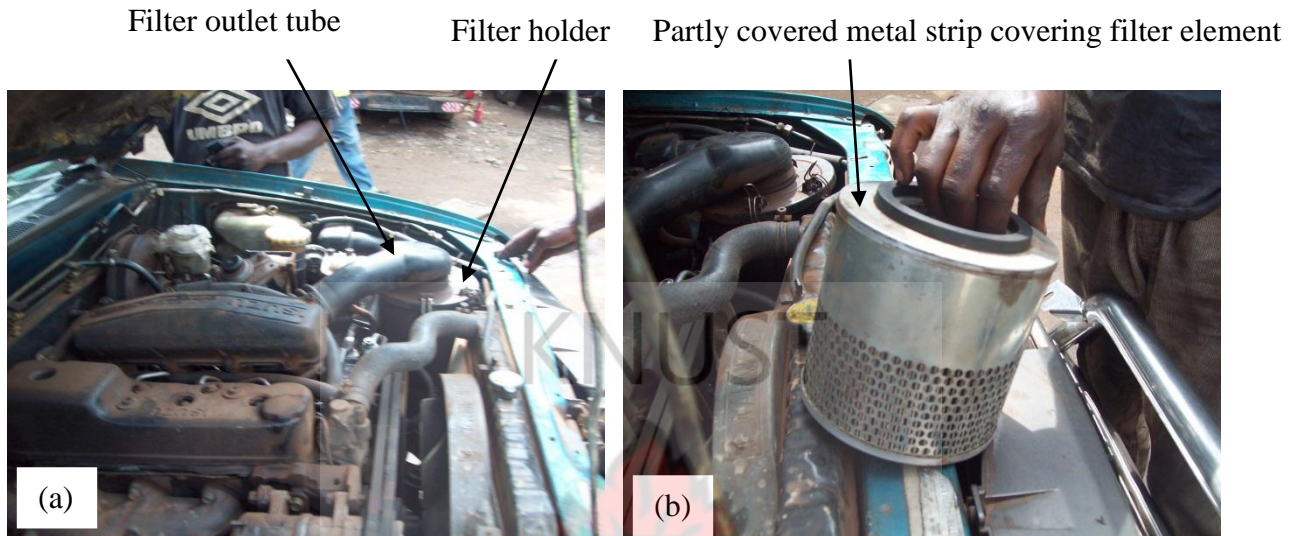


Figure 2.25 (a) Isuzu KB filter holder.(b) Isuzu KB filter element

2.4.7 Mazda 626

The inlet tube of the filter holder has its opening at the front of the vehicle. The filter holder is located to the right and mid-way of the engine compartment shown in Figure 2.26 (a). The filter element is a panel style type made of paper as shown in Figure 2.26 (b). Since the engine is a petrol type, it is equipped with an air flow sensor.

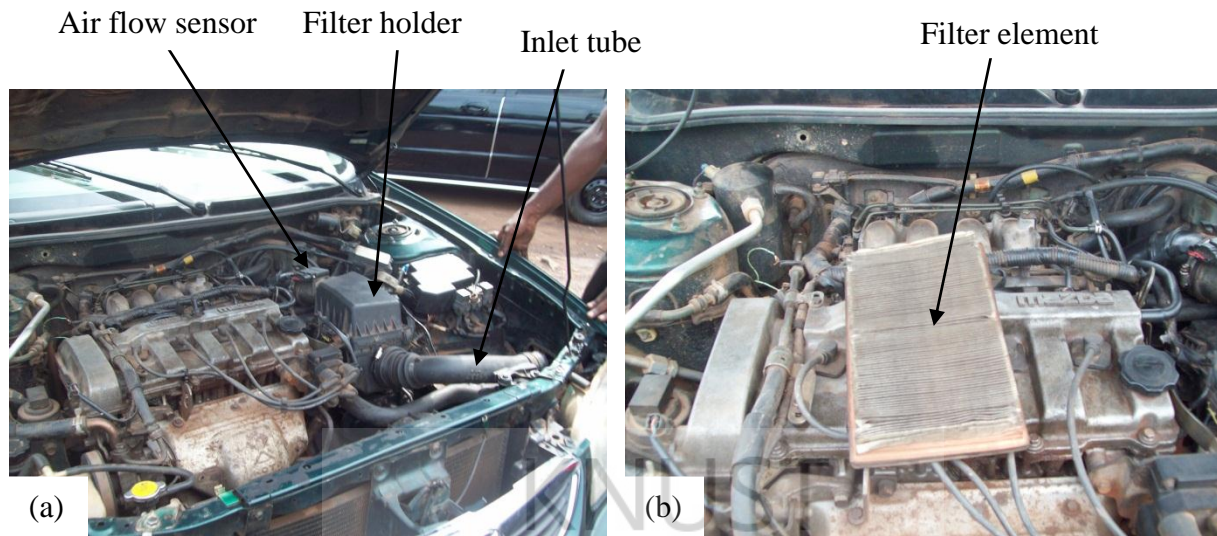


Figure 2.26 (a) Mazda 626 filter holder with inlet tube. (b) Mazda 626 filter element

2.4.8 Nissan Maxima

A panel style paper filter element shown in Figure 2.27 (b) is used in this petrol engine vehicle. The filter holder is placed to the right and mid-way of the engine compartment shown in Figure 2.27 (a). The inlet tube has its opening facing down. The air flow quantity after filtration is monitored by an air flow sensor.

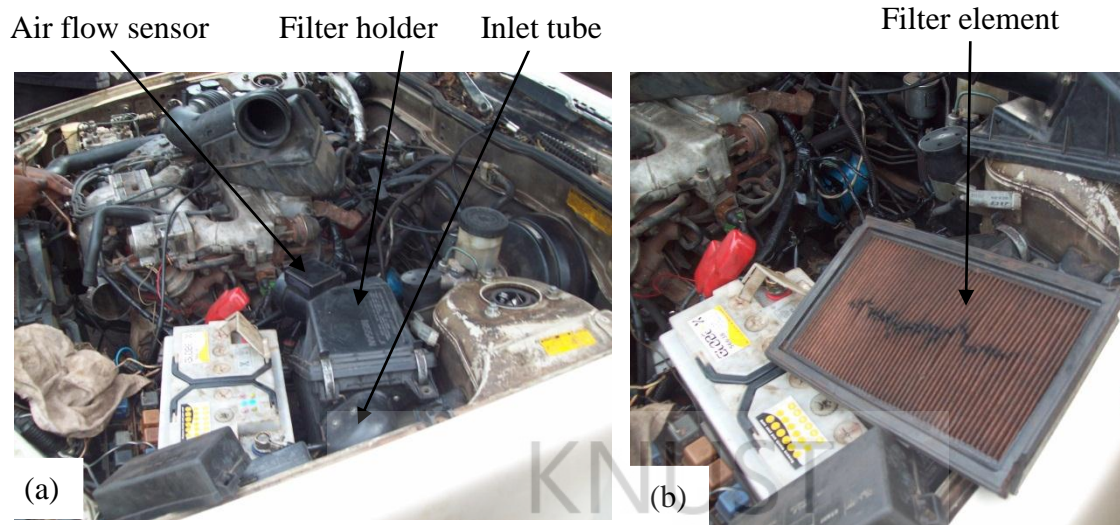


Figure 2.27 (a) Nissan Maxima filter holder. (b) Nissan Maxima filter element

2.4.9 Nissan Micera

The engine block and the filter holder are placed close to each other. The filter holder shown in Figure 2.28 (a) is located after the engine block and to the far end of the vehicle. The inlet tube is a long one with its opening to the right of the vehicle. The filter element shown in Figure 2.28 (b) is a paper type that occupies the inclined portion of the holder. The inclined arrangement helps some aerosol particles to settle by gravity. The outlet tube has its opening covered with a sieve. This prevents very tiny atmospheric aerosols that may still pass through the filter from entering the engine.

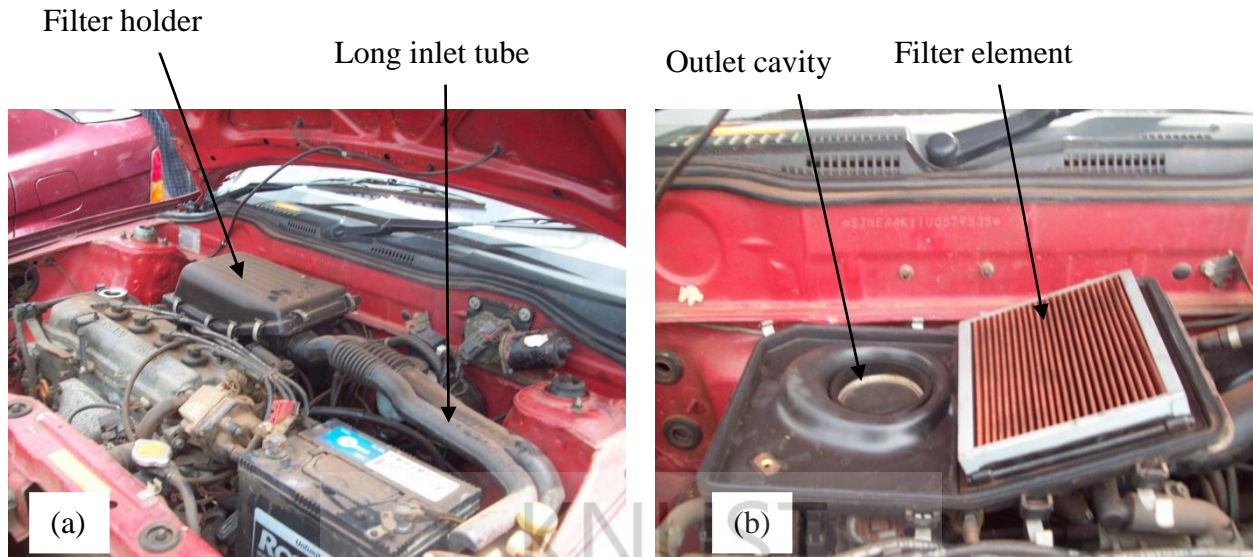


Figure 2.28 (a) Nissan Micera filter holder with inlet tube. (b) Nissan Micera filter element

2.4.10 Nissan Urvan

A cylindrical filter element is fitted in this vehicle. A metallic strip covers the element as shown in Figure 2.29 (b). The metal cover blocks some atmospheric aerosols from entering the filter. The openings created allow more air to enter for combustion. The filter element is a paper type. Atmospheric aerosol filtered off settles in a plastic container around the filter element and inside the holder shown in Figure 2.29 (a). Air enters the filter element from under the vehicle.

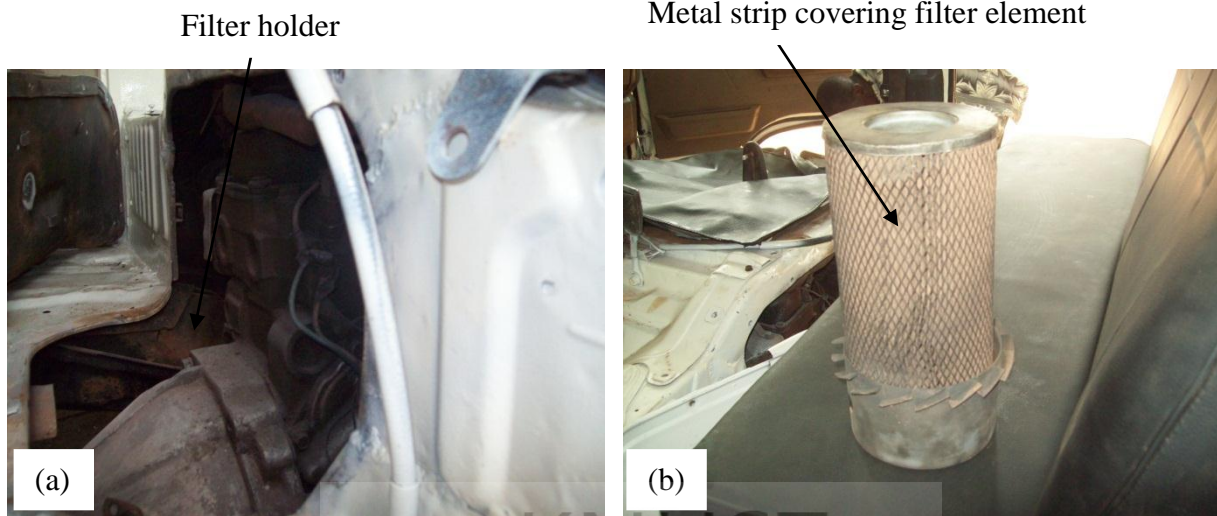


Figure 2.29 (a) Nissan Urvan filter holder. (b) Nissan Urvan filter element

2.4.11 Opel Daewoo Leganza

The filter holder is located behind the engine block and is circular in shape as shown in Figure 2.30 (a). The inlet tube is a long one with its opening in the engine compartment. The filter element is made of paper as shown in Figure 2.30 (b).

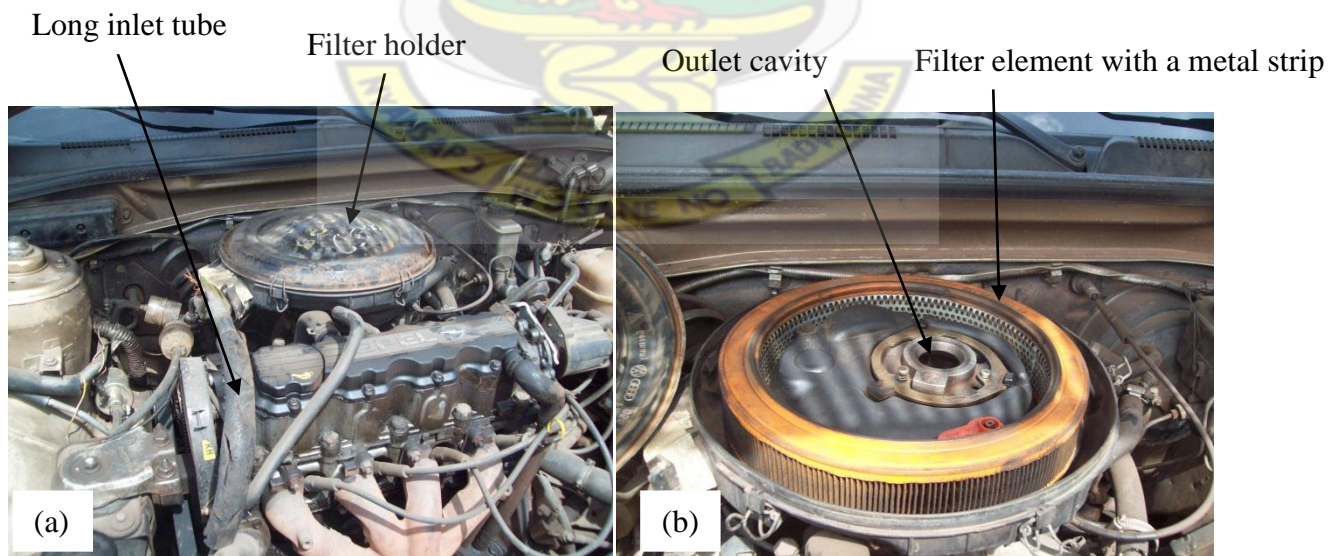


Figure 2.30 (a) Opel Daewoo Leganza filter holder. (b) Opel Daewoo Leganza filter element

2.4.12 Opel Vectra

A panel style paper filter shown in Figure 2.31 (b) is used in this vehicle. The filter holder is placed to the far left of the engine compartment as shown in Figure 2.31 (a) and is close to the engine. The inlet tube opening is close to the front of the vehicle.

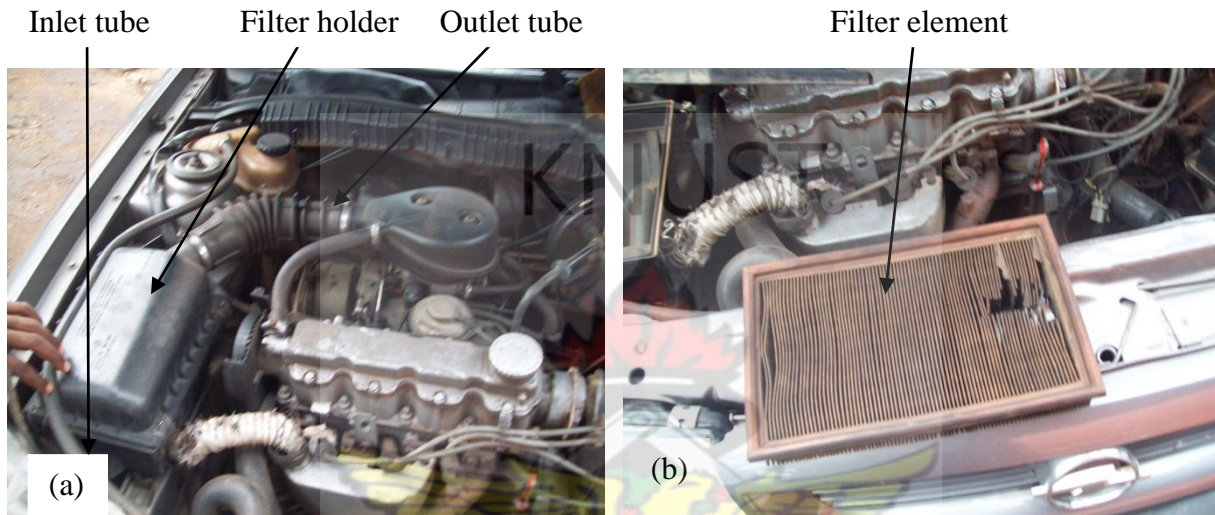


Figure 2.31 (a) Opel Vectra filter holder.

(b) Opel Vectra filter element

2.4.13 Toyota Coaster

It uses a two-layered panel style paper filter shown in Figure 2.32 (b) placed in a holder located just around the centre of the engine compartment and close to the engine block. The filter holder shown in Figure 2.32 (a) has a short inlet tube. The filter holder uses an air flow sensor.

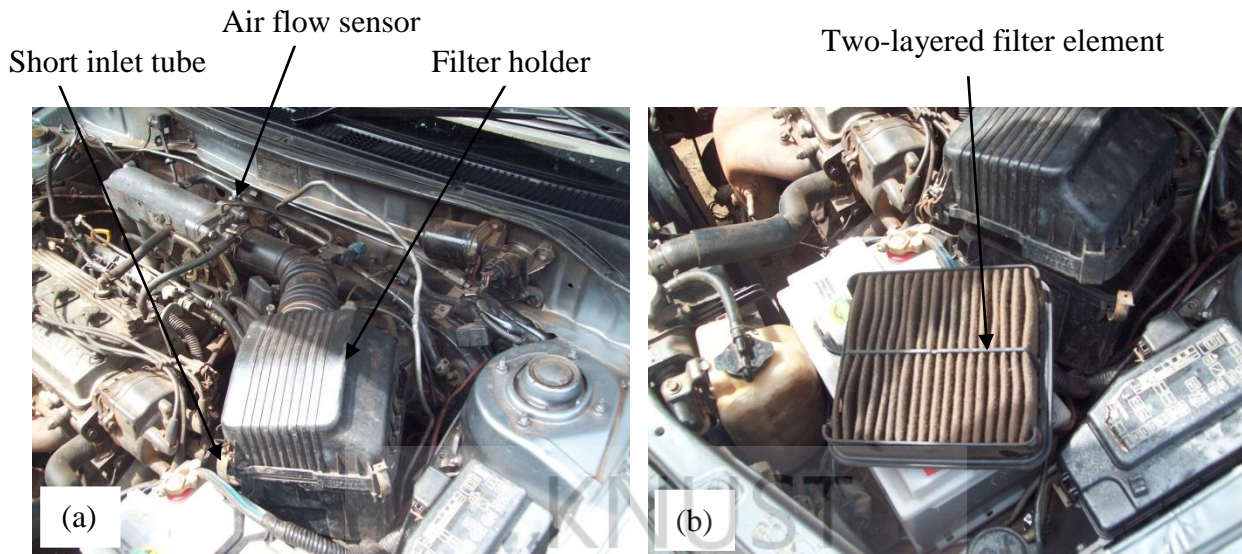


Figure 2.32 (a) Toyota Coaster filter holder. (b) Toyota Coaster filter element

2.4.14 Toyota Carina e

It uses a paper filter shown in Figure 2.33 (b) placed in a holder shown in Figure 2.33 (a) located just around the centre of the engine compartment and close to the engine block. The filter holder has a short inlet tube. The filter holder uses an air flow sensor.

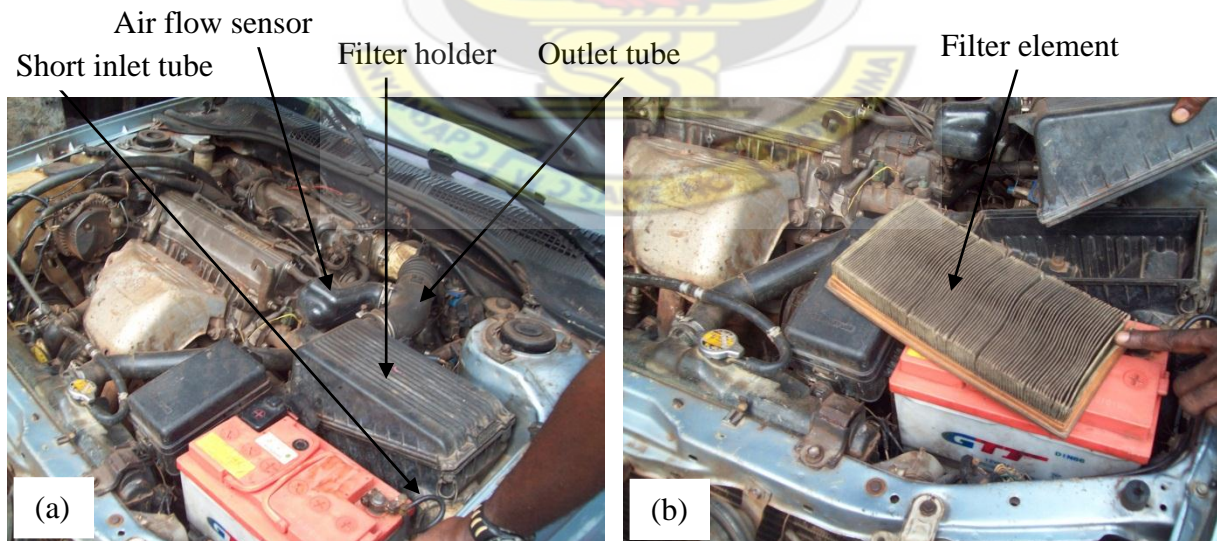


Figure 2.33 (a) Toyota Carina e filter holder. (b) Toyota Carina e filter element

2.4.15 Toyota Corolla LE/CE

It uses a two-layered panel style paper filter shown in Figure 2.34 (b) placed in a holder shown in Figure 2.34 (a) located just around the centre of the engine compartment and close to the engine block. The filter holder has a short inlet tube. The filter holder uses an air flow sensor.

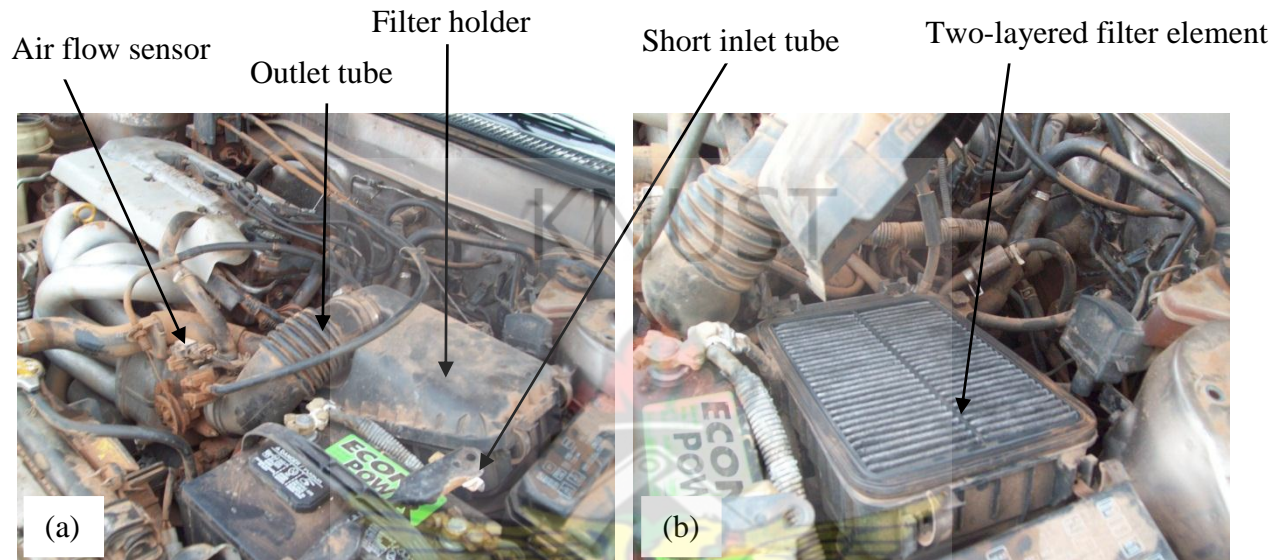


Figure 2.34 (a) Toyota Corolla LE/CE filter holder. (b) Toyota Corolla LE/CE filter element

2.4.16 Toyota Tercel

It uses a two-layered panel style paper filter shown in Figure 2.35 (b) placed in a holder shown in Figure 2.35 (a) located close to the rear end of the engine compartment and close to the engine block. The filter holder has a short inlet tube. The filter holder uses an air flow sensor.

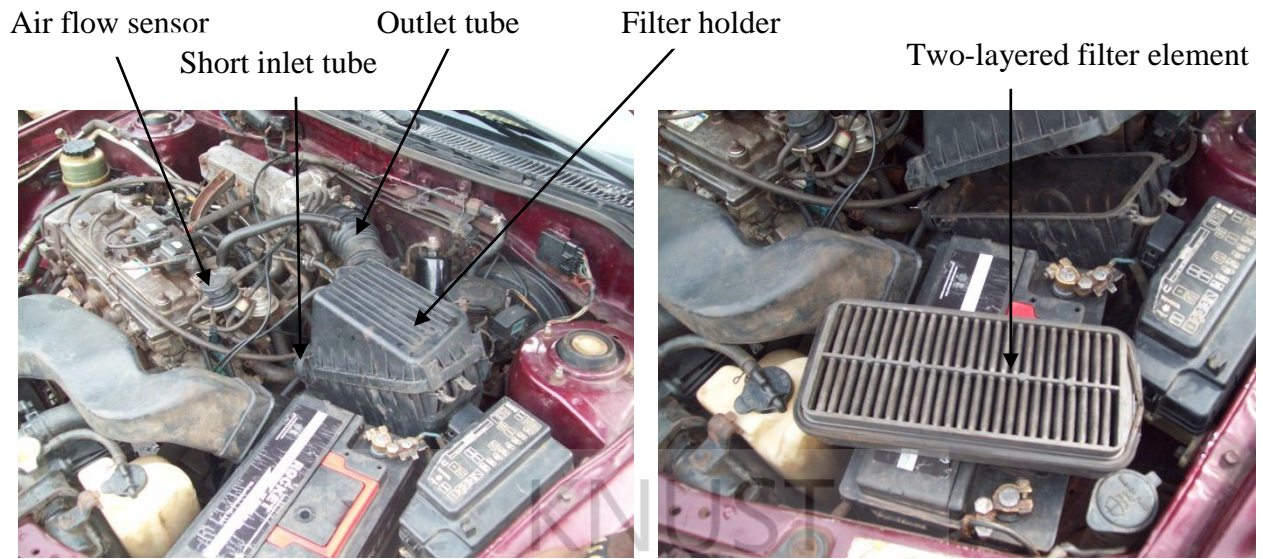


Figure 2.35 (a) Toyota Tercel filter holder. (b) Toyota Tercel filter element

2.4.17 Toyota Tundra

The filter holder shown in Figure 2.36 (a) is placed to the left and front of the engine compartment. It uses a three-layered panel style foam filter shown in Figure 2.36 (b).

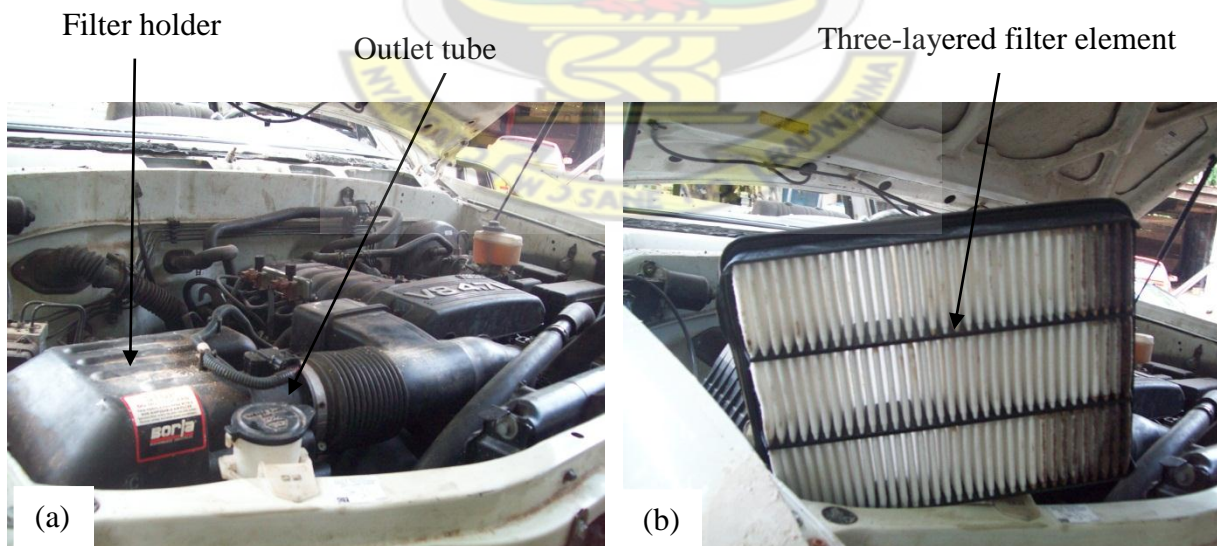


Figure 2.36 (a) Toyota Tundra filter holder. (b) Toyota Tundra filter element

2.4.18 Volvo 460

The filter holder is located behind the engine block and is circular in shape as shown in Figure 2.37 (a). The inlet tube is a short one with its opening in the engine compartment. The filter element is made of paper as shown in Figure 2.37 (b).

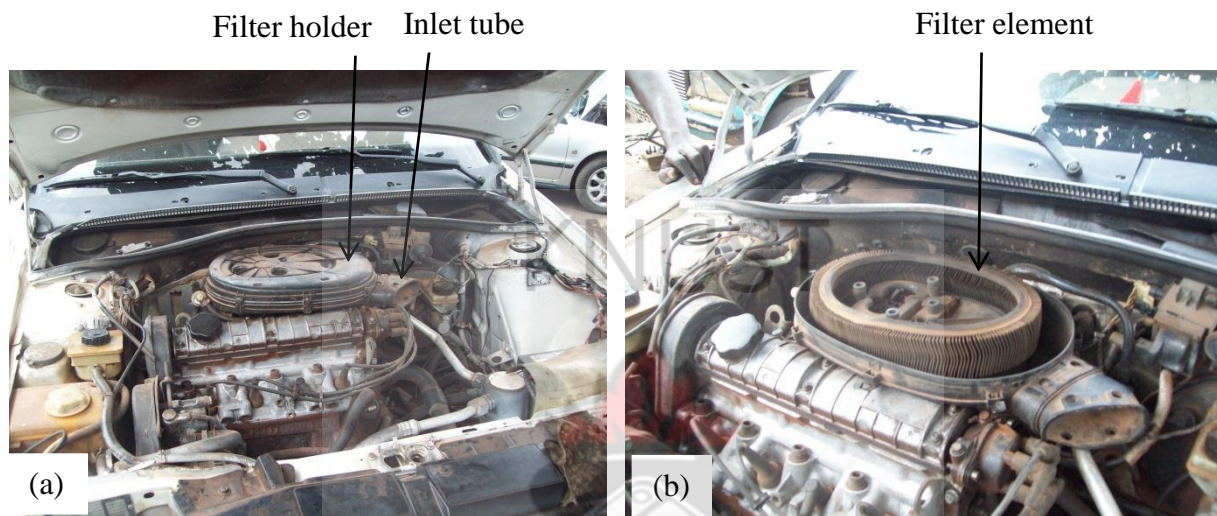


Figure 2.37 (a) Volvo 460 filter holder with inlet tube. (b) Volvo 460 filter element

2.4.19 Volvo S40

The filter holder is located to the right of the engine compartment and is in line with the engine block as shown in Figure 2.38 (a). It has a panel paper type filter shown in Figure 2.38 (b) and uses an air flow sensor.

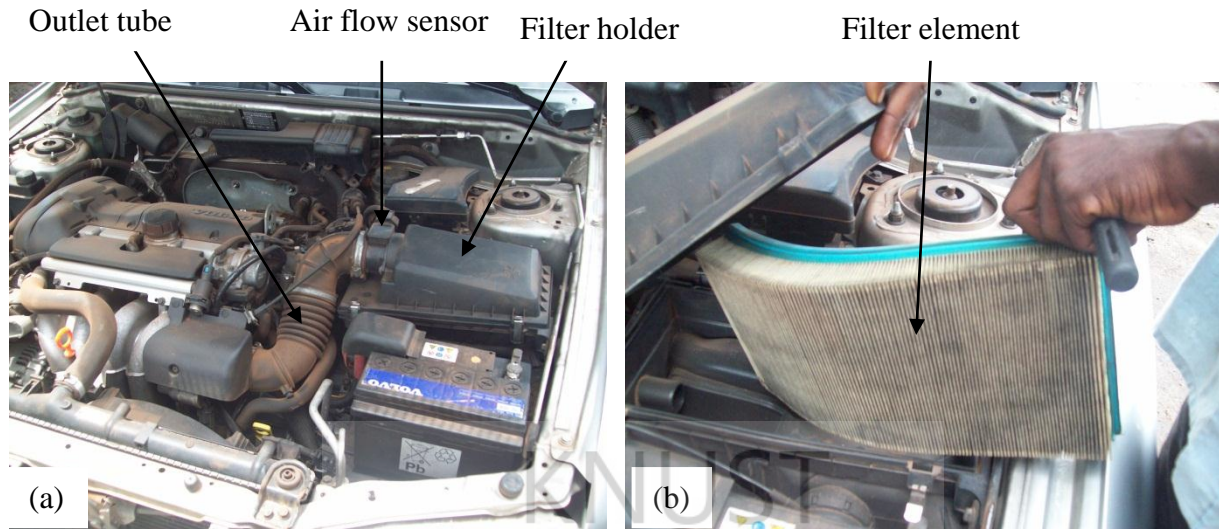


Figure 2.38 (a) Volvo S40 filter holder.

(b) Volvo S40 filter element

2.4.20 Volvo S60

The filter holder shown in Figure 2.39 (a) is located to the right and front of the engine compartment. The inlet tube has its opening attached to the front of the vehicle. It uses a paper type panel filter style shown in Figure 2.39 (b).

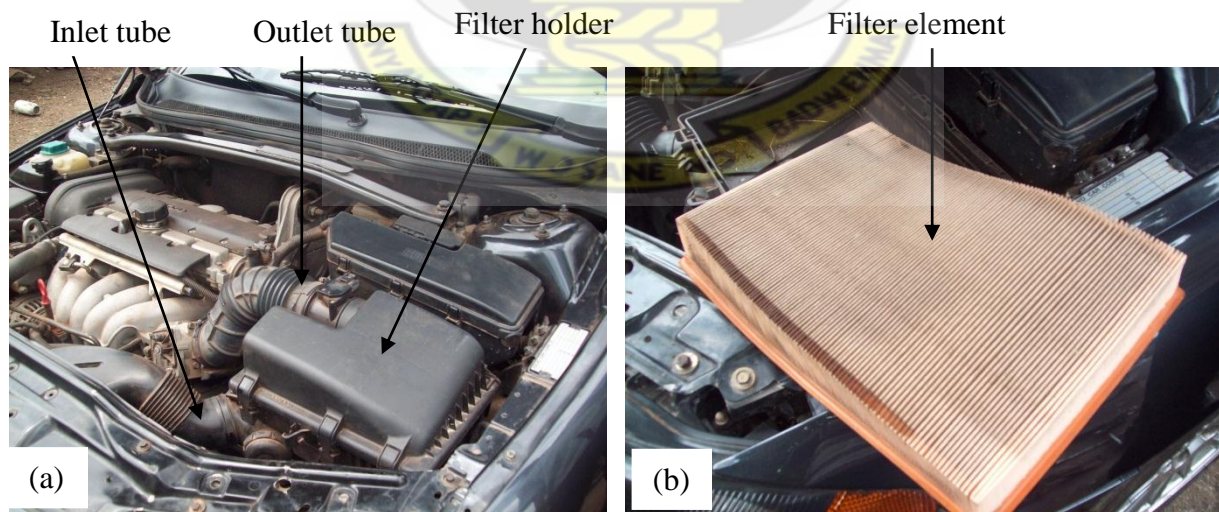


Figure 2.39 (a) Volvo S60 filter holder.

(b) Volvo S60 filter element

2.4.21 VW Golf 4

The filter holder of this vehicle is located to the right and rear of the engine compartment. The filter holder is fixed in place in an inclined manner as shown in Figure 2.40 (a). This causes heavier aerosol particles to settle by gravity as they pass through the filter. The filter element shown in Figure 2.40 (b) is also covered with foam across its entire length; this increases filtration efficiency.

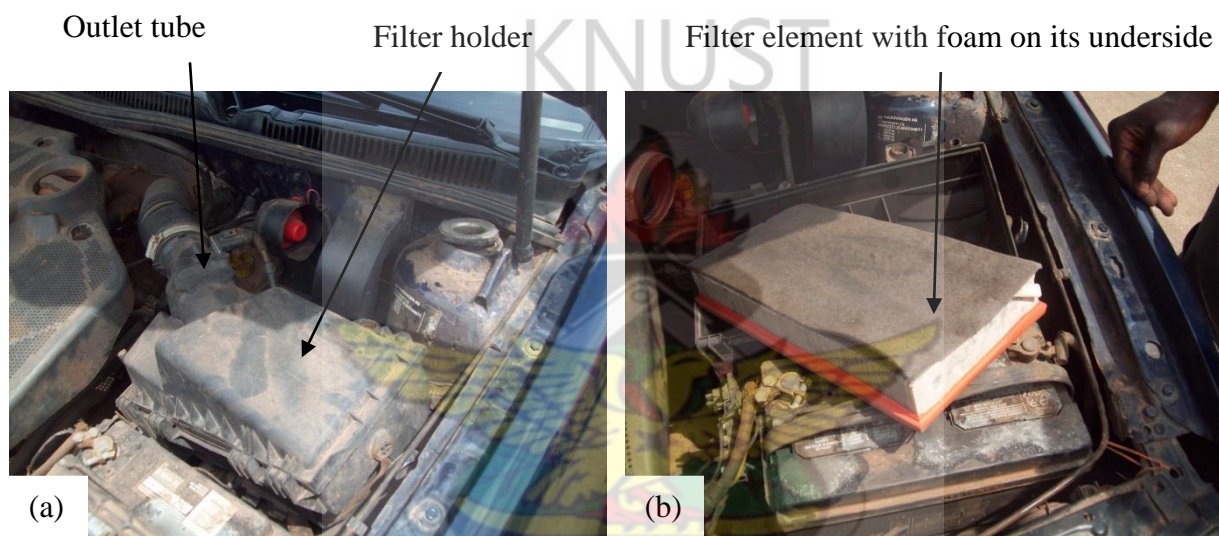


Figure 2.40 (a) VW Golf 4 filter holder.

(b) VW Golf 4 filter element

CHAPTER THREE

EXPERIMENTAL SET-UP AND PROCEDURE

The Harmattan aerosol constitutes the ambient air during the Harmattan period, which lasts about five months in most parts of Ghana and West Africa. It is the air that is sucked in for combustion in vehicles and breathing. The average dust particle sizes range from about 0.89 μm to about 2.43 μm . The mass concentrations range between 168 $\mu\text{g}/\text{m}^3$ and 1331 $\mu\text{g}/\text{m}^3$ (Sunnu et al, 2006). The high concentration of dust particles during the Harmattan impacts on vehicle engine performance. It also reduces the filter life. The following experiment is aimed at determining the effects of dust on combustion filters of vehicles in relation to engine performance. The descriptions of the various components of the set-up and the experimental procedure are also presented here.

3.1 Experimental set-up

Experiments were conducted using the set-up shown in Figure. 3.1, which is aimed at determining the effect of dusty Harmattan air on the performance of the vehicle engine. The set-up consists of a big transparent plastic bottle placed on a platform which is about 76 cm high. The platform consists of a table with a plastic container placed on top. A box of paper was then placed on the container and a drawing board on top of the box. This arrangement was made in order to give the required height to support the plastic gallon. Holes were made with the edge of a screw driver around the base of the plastic bottle. The diameter of the holes was approximately 0.4 cm. The plastic bottle was covered with its lid at the top. This arrangement created air-dust circulation in the gallon. A plane white paper was placed underneath the bottle to collect any dust samples that escaped through the holes.

A hole of approximately 6 cm diameter equal to the diameter of the inlet tube of the filter holder was made on one side of the bottle. The hole on the bottle and the inlet tube cavity were then connected using a plastic hose of slightly larger diameter. To avoid air and dust leakages from the plastic bottle, the plastic hose was sealed with epoxy. Similarly, a metal clip was used to tighten the plastic hose onto the inlet tube of the holder.

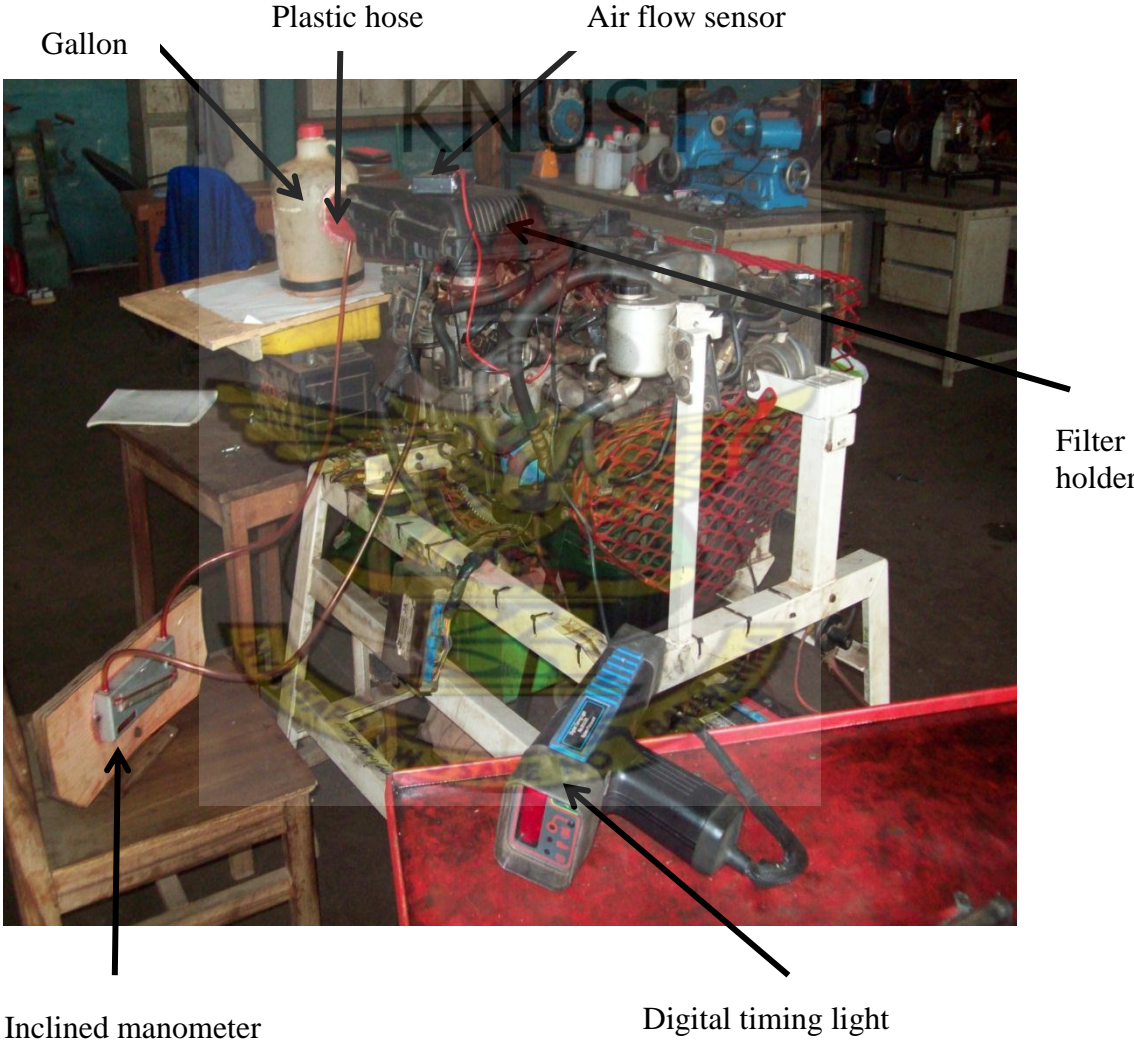


Figure 3.1: Experimental set-up

The set-up was also equipped with an air flow sensor to monitor the air volume entering the engine with time. In order to record the engine speed as dust loading continued, a digital timing light was used. The red wire of the timing light was connected to the positive terminal of the battery while the black wire was connected to the negative terminal. The digital timing light also had a crocodile clip which was connected to the number 1 spark plug cable. Sensors in the clip determine the time current enters spark plug 1 so that the engine speed recorded will be more accurate. The fuel level was recorded before and after the various processes. The set-up was also equipped with an inclined manometer with paraffin to measure the pressure drop across the filter assembly. The schematic diagram of the experimental set-up is shown in Figure 3.2.

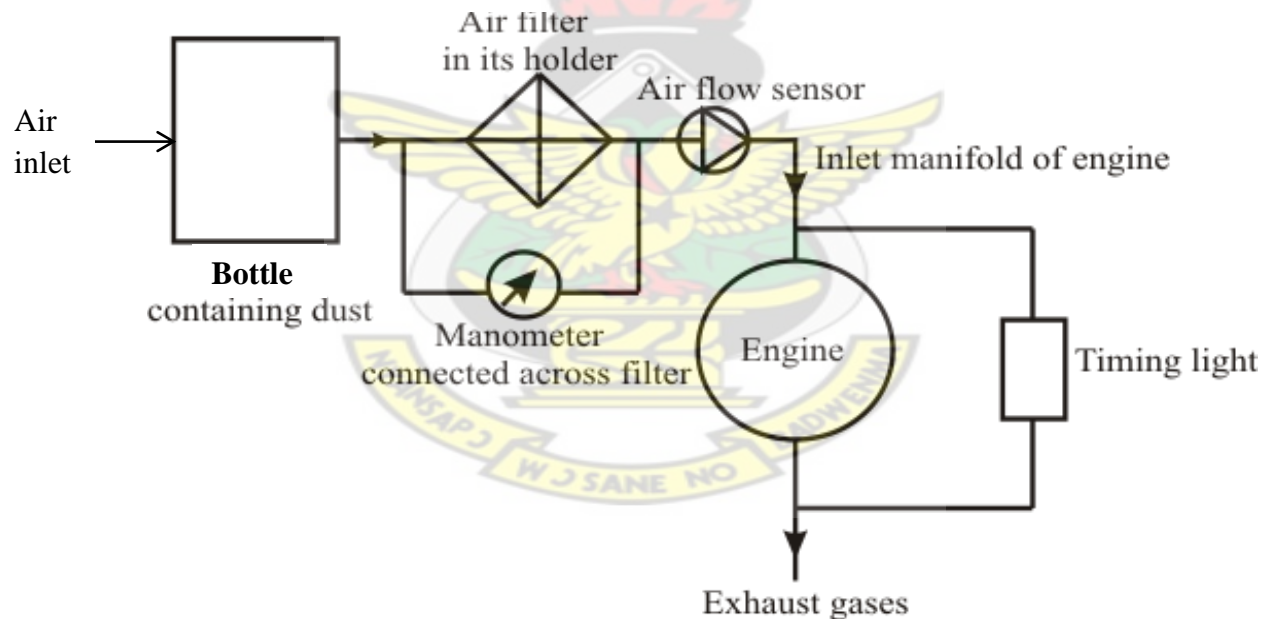


Figure 3.2: Schematic diagram of the Experimental set-up

Three different filters (shown in Figure 3.3) were involved in the investigation. The main parameters and dimensions of these filters are presented in Table 3.1. Yellow foam filter has a pore size of $2\ \mu\text{m}$, the paper filter has a pore size of $2\ \mu\text{m}$ and the red foam filter has a pore size

of 1 μm . These values were provided by the manufacturers. The volume fraction of fibers, called the packing density or solidity, for the filters is shown in appendix II. The filters have been chosen to have similar parameters for the most representative comparison.

Table 3.1 Parameters of filters

Filter number	Filter material	Fibre distance (cm)	Thickness of fibre (cm)	Breadth of fibre (cm)	Height of fibre (cm)	Breadth of filter (cm)	Length of filter (cm)	Height of filter (cm)	Number of fibres
1	Foam	0.20	0.1	13.8	2.3	15	20.3	3.8	58
2	Foam	0.25	0.15	14.5	1.6	16.9	27.9	3.5	52
3	Paper	0.25	0.1	14.5	1.6	16.5	27.7	3.5	62

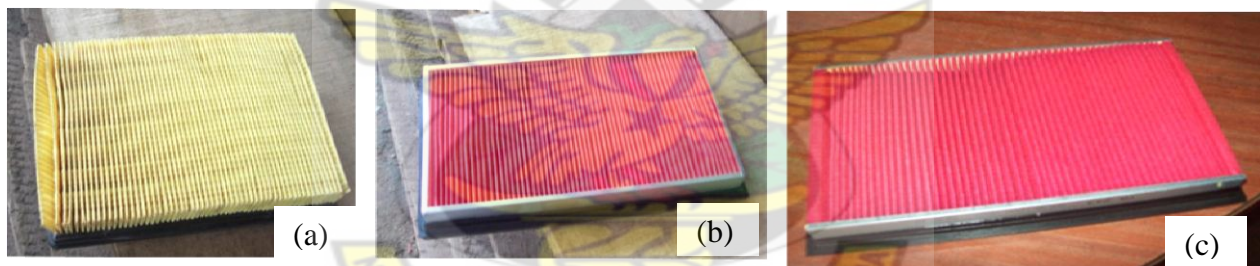


Fig. 3.3: (a) Foam Filter (b) Paper Filter (c) Foam Filter

3.2 Experimental procedure

The first step of the experimental programme was the collection of dust samples. Inflated dust from an untarred road was collected using four plastic sheeting materials along an unpaved road (Dr. Brobbey junction, Kotei) in Kumasi between February 10 and February 17, 2011. The plastic materials were placed on tables along the road around 11 am each day. Stones were placed on the corners of the sheets to provide support. The plastic sheets were then collected around 4 pm and the dust samples were stored in plastic bottles. Settling Harmattan dust was also

collected from the roof top of the College of Engineering new classroom and laboratory blocks between February 10 and February 17, 2011. Four plastic sheeting materials were used to collect these samples. The plastic materials were placed around 12 pm each day and collected around 3 pm, so that the other plastic sheets placed around 11 am can be collected around 4 pm. The dust samples were also stored in plastic gallons. The dust collected by the side of the untarred road represented the dust effect on vehicles running on untarred roads while the dust collected on top of the laboratory represented the dust effect on vehicles running on tarred roads.

Six different 250 ml plastic bottles were used to keep the dust samples. The bottles were grouped into two and each group contained the same mass of dust. The mass of dust in both groups was 529 g. The masses of the three different air filters were measured and recorded. Each filter was placed in its holder and connected to the engine block. In order to obtain a representative comparison, each filter was tested (using the experimental set-up in Figure 4.1) two times. The average dust loading rates were 0.08 g/s and 0.14 g/s (calculations shown in appendix I) for idling conditions of the engine. In order to investigate the rate of clogging of each filter, the pressure drop was continuously monitored at 0, 1, 2, 3, 4 and 5 minutes after starting the process. Each sampling filter was weighed before and after sampling and the dust arrestance/collection efficiency (appendix I) by the filter was then calculated. For the final series of measurements, the engine speed and the air flow rate from the filter into the engine were also recorded at the same time interval. The fuel level before and after each test was also recorded.

The results of values obtained from the experimental procedure are presented in tables and their corresponding graphs in chapter four. Calculations showing the dust loading rate, the dust

arrestance/collection efficiency of the filters and the packing density of the filters are also shown in (appendix I and II respectively).

KNUST



CHAPTER FOUR

RESULTS AND DISCUSSIONS

The results of the experiment are presented and discussed in this chapter.

4.1 Results

The results of measurement of the yellow foam filter tested for different dust loading rates of 0.08 g/s and 0.14 g/s are presented in Tables 4.1 (a) and (b).

Table 4.1 (a): Results of experimental measurements for roof top dust (at 0.08 g/s) for the yellow foam filter.

Time (mins)	Engine speed, rpm	Air flow, V	ΔP (inches of paraffin)	ΔP (m of paraffin)	ΔP (Pa)
0	0.00	0.00	0.00	0.0000	0.000
1	1580	1.72	0.13	0.0033	7.577
2	1570	1.71	0.13	0.0034	7.810
3	1560	1.71	0.14	0.0034	7.868
4	1560	1.70	0.14	0.0035	8.043
5	1550	1.69	0.14	0.0035	8.101

Table 4.1 (b): Results of experimental measurements for untarred road dust (at 0.14 g/s) for the yellow foam filter.

Time (mins)	Engine speed, rpm	Air flow, V	ΔP (inches of paraffin)	ΔP (m of paraffin)	ΔP (Pa)
0	0.00	0.00	0.00	0.00	0.000
1	3400	0.79	0.32	0.0080	18.359
2	2900	0.76	0.35	0.0089	20.398
3	2700	0.75	0.35	0.0089	20.398
4	2700	0.75	0.37	0.0093	21.418
5	2700	0.74	0.37	0.0093	21.418

The corresponding graph showing the results of monitoring of the resistance of the filter utilized in dust removal with respect to time for the different dust loading rates is also shown in Figure 4.1 (a). Similar graphs for the same filter showing the air flow after the filter and the engine speed with respect to time are also shown in Figures 4.1 (b) and 4.1 (c).



Figure 4.1(a): Pressure drop against time for the yellow foam filter.

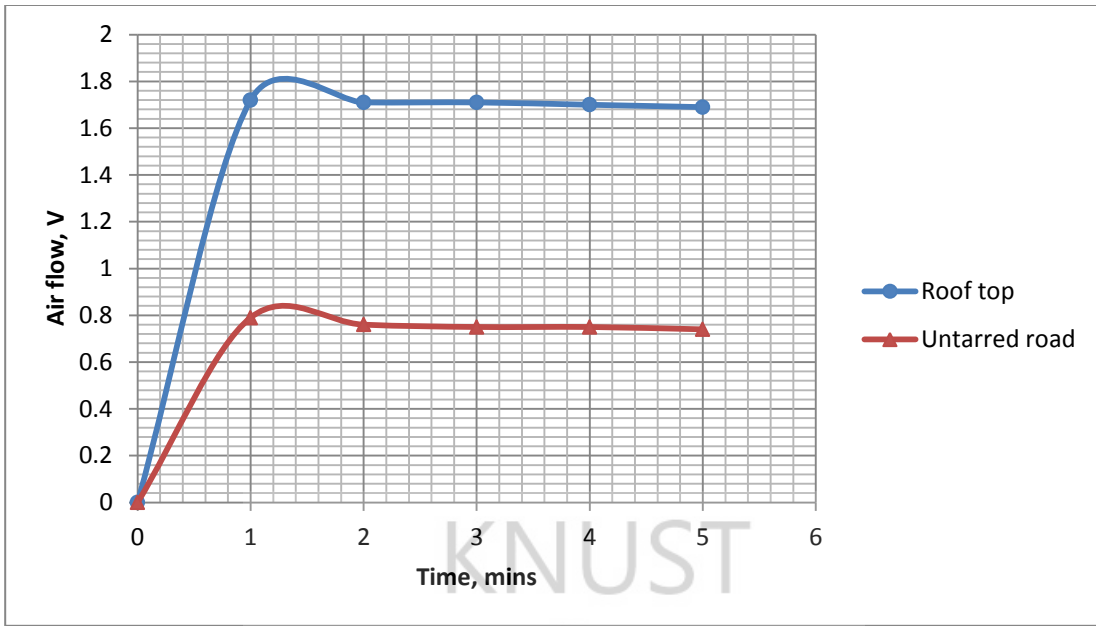


Figure 4.1 (b): Air flow against time for the yellow foam filter.

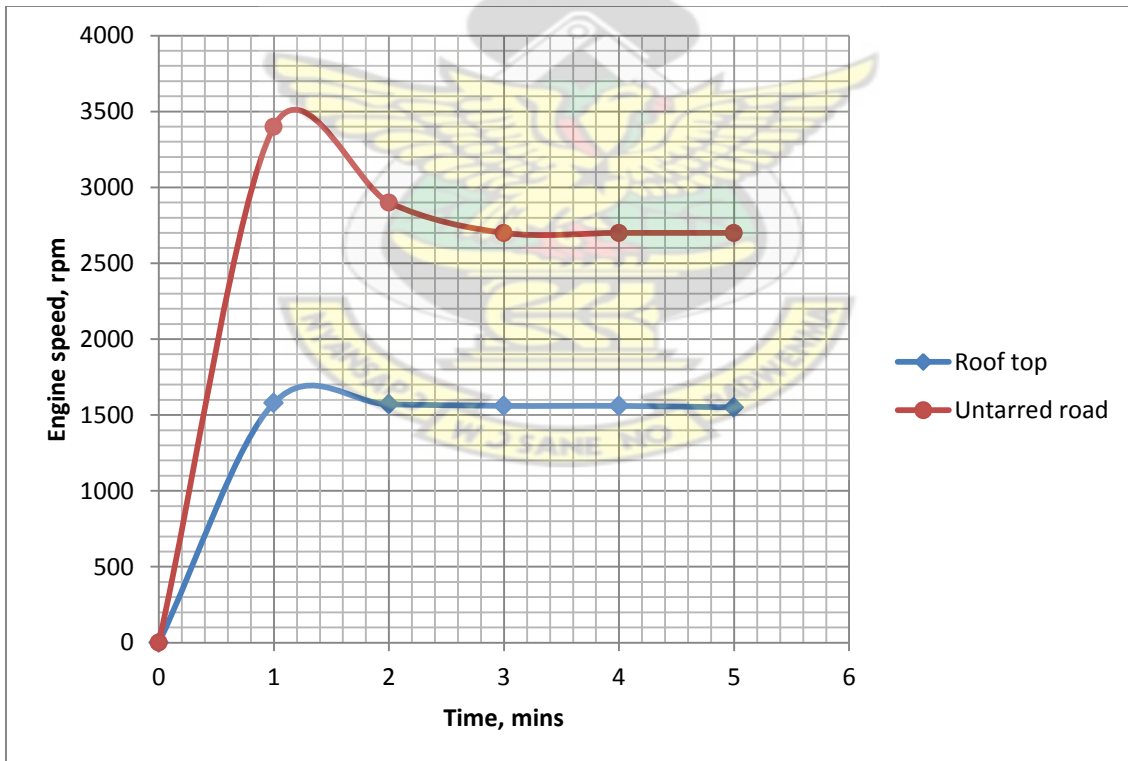


Figure 4.1 (c): Engine speed against time for the yellow foam filter.

The results of the same measurements (engine rpm, air flow and pressure drop) for the other two filters (the paper filter and the red foam filter) are also presented.

Table 4.2 (a): Results of experimental measurements for roof top dust (at 0.08 g/s) for the paper filter.

Time (mins)	Engine speed, rpm	Air flow, V	ΔP (inches of paraffin)	ΔP (m of paraffin)	ΔP (Pa)
0	0.00	0.00	0.00	0.00	0.000
1	1190	1.29	0.17	0.0044	10.100
2	1180	1.28	0.18	0.0045	10.410
3	1170	1.28	0.18	0.0046	10.488
4	1170	1.28	0.18	0.0047	10.721
5	1160	1.27	0.19	0.0047	10.799

Table 4.2 (b): Results of experimental measurements for untarred road dust (at 0.14 g/s) for the paper filter.

Time (mins)	Engine speed, rpm	Air flow, V	ΔP (inches of paraffin)	ΔP (m of paraffin)	ΔP (Pa)
0	0.00	0.00	0.00	0.00	0.000
1	6800	0.74	0.30	0.0077	17.653
2	6700	0.73	0.31	0.0079	18.197
3	6700	0.73	0.31	0.0080	18.332
4	6700	0.73	0.32	0.0082	18.740
5	6600	0.72	0.32	0.0082	18.876

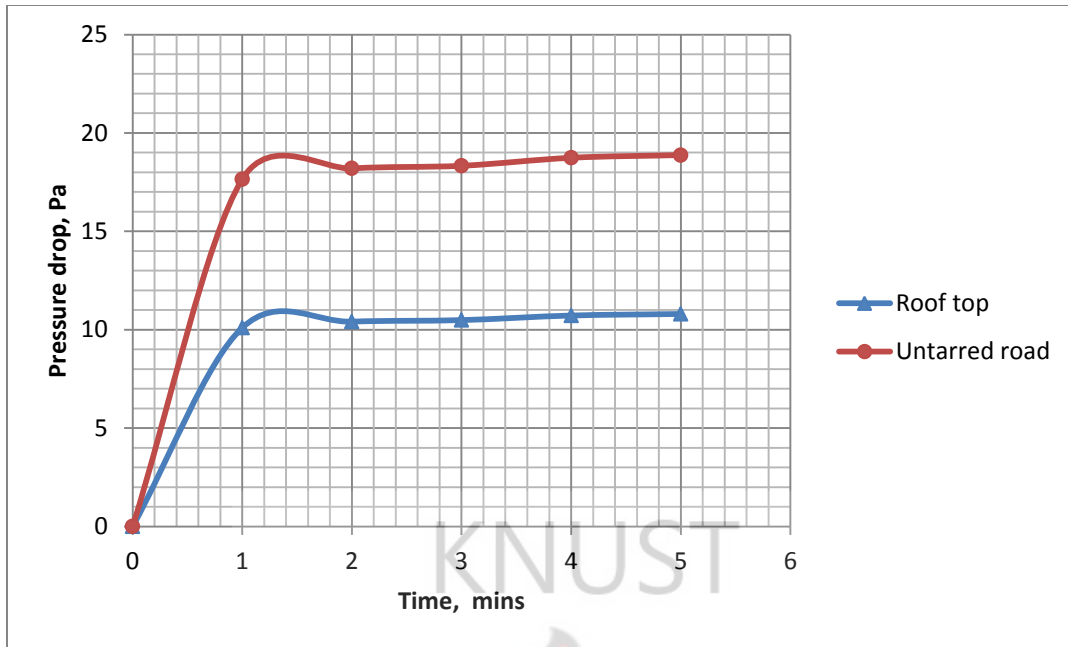


Figure 4.2 (a): Pressure drop against time for the paper filter.

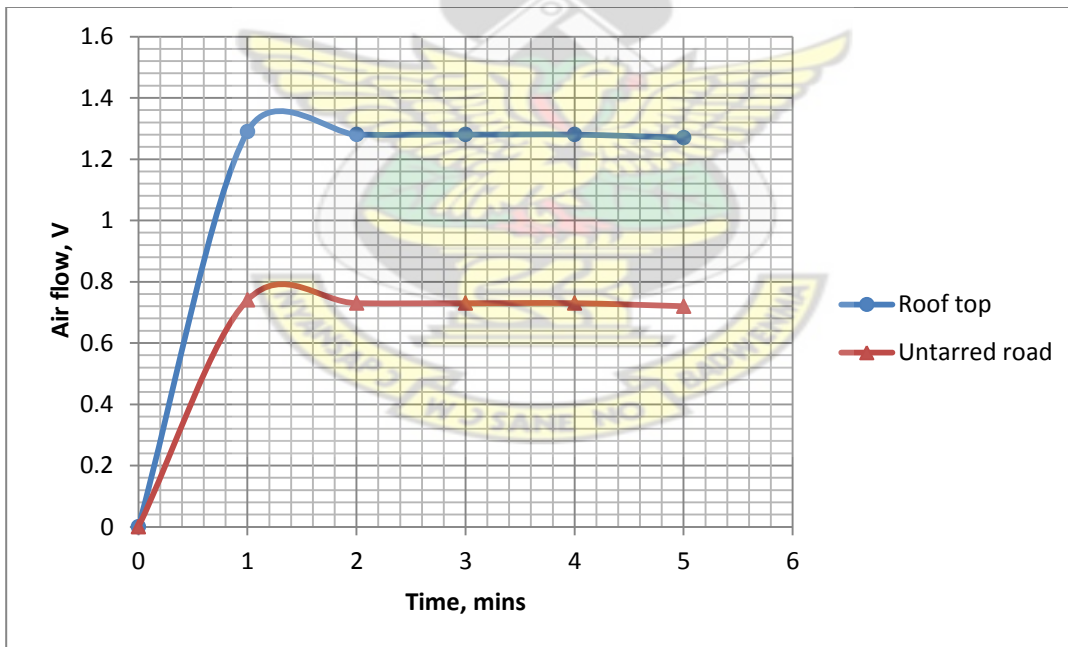


Figure 4.2 (b): Air flow against time for the paper filter.

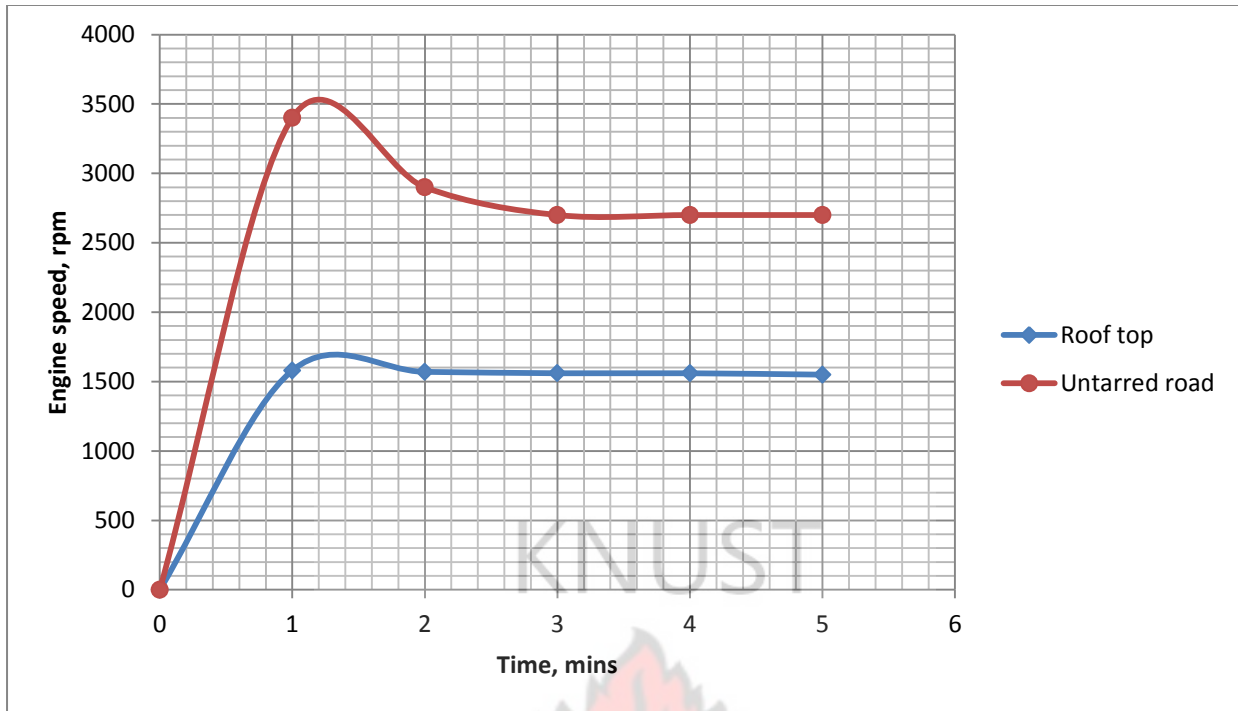


Figure 4.2 (c): Engine speed against time for the paper filter.

Table 4.3 (a): Results of experimental measurements for roof top dust (at 0.08 g/s) for the red foam filter.

Time (mins)	Engine speed, rpm	Air flow, V	ΔP (inches of paraffin)	ΔP (m of paraffin)	ΔP (Pa)
0	0.00	0.00	0.00	0.00	0.000
1	1370	1.65	0.58	0.0147	33.803
2	1360	1.65	0.58	0.0147	33.803
3	1350	1.63	0.6	0.0152	34.969
4	1330	1.63	0.6	0.0152	34.969
5	1320	1.62	0.61	0.0155	35.551

Table 4.3 (b): Results of experimental measurements for untarred road dust (at 0.14 g/s) for the red foam filter.

Time (mins)	Engine speed, rpm	Air flow, V	ΔP (inches of paraffin)	ΔP (m of paraffin)	ΔP (Pa)
0	0.00	0.00	0.00	0.00	0.000
1	7800	0.94	1.02	0.0258	59.155
2	7800	0.94	1.02	0.0258	59.155
3	7700	0.93	1.05	0.0267	61.195
4	7600	0.93	1.05	0.0267	61.195
5	7500	0.93	1.07	0.0271	62.215

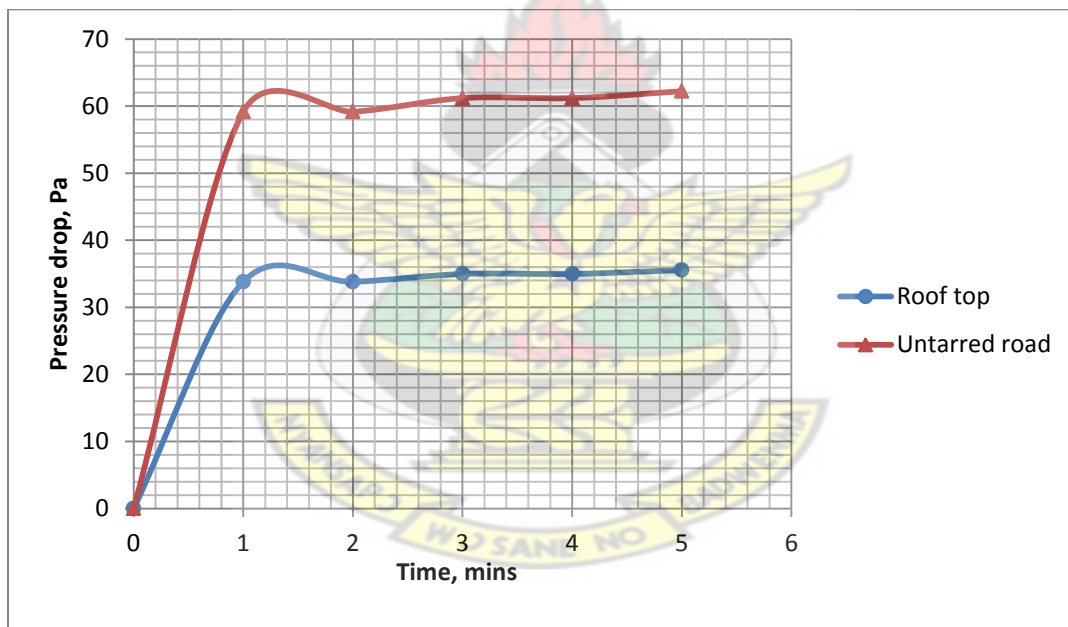


Figure 4.3 (a): Pressure drop against time for the red foam filter.

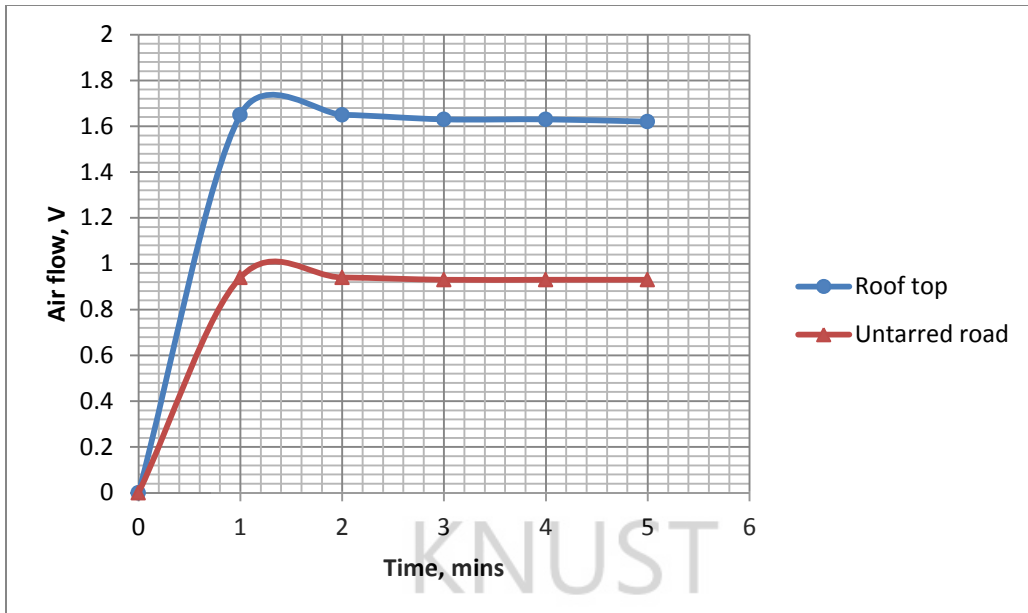


Figure 4.3 (b): Air flow against time for the red foam filter.

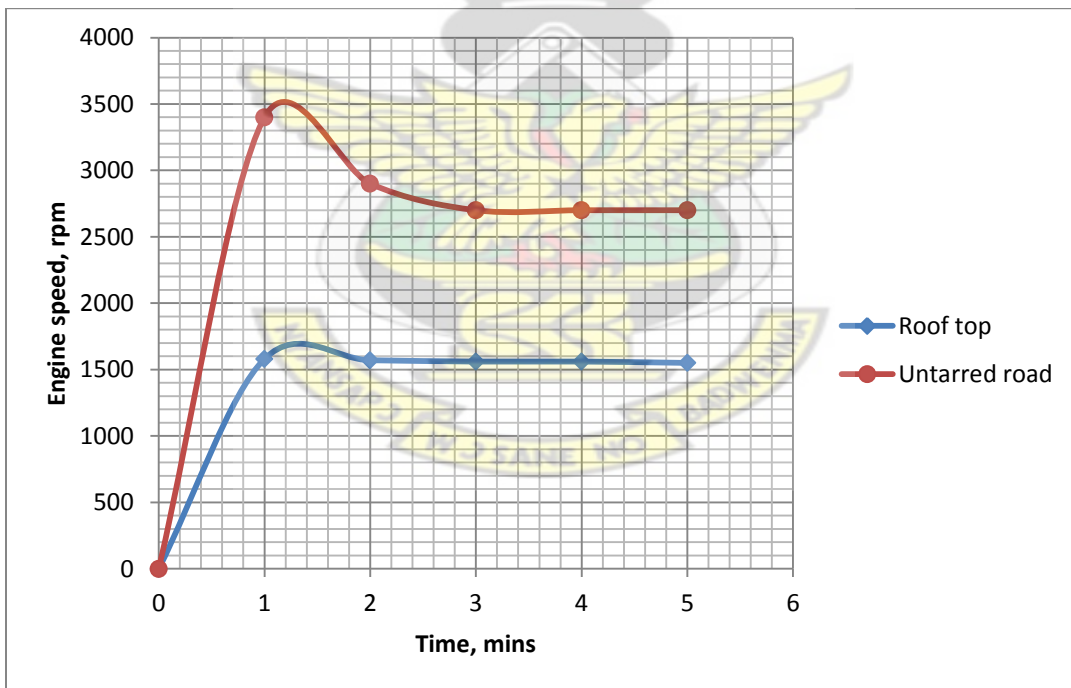


Figure 4.3 (c): Engine speed against time for the red foam filter.

Results from the measurements of the three different filters clearly show that the pressure drop varies linearly with time within one minute after the start of the process. However, for the dust

collected on the roof top at 0.08 g/s dust loading rate, the resistance (a measure of the pressure drop) for the paper filter was approximately 2 times more compared to the yellow foam filter whilst that of the red foam filter was 26 times more compared to the yellow foam filter, after one minute of the process. For the dust collected on the untarred road, the resistance of the paper filter was approximately the same compared to the yellow foam filter. The resistance of the red foam filter was 44 times more compared to the yellow foam filter, after one minute of the process. The results also indicate that the air flow over yellow foam filter for the dust collected on the roof top at 0.08 g/s dust loading was approximately 0.4 times more and 0.1 times more compared to the paper filter and the red foam filter within the same interval. For the dust on the untarred road, the air flow after the yellow foam filter was 0.1 times more compared to the paper filter whilst that of the red foam filter was 0.2 times more compared to the yellow foam filter.

Also, the engine speed for the dust collected on the roof top at 0.08 g/s dust loading for the yellow foam filter was approximately 0.4 times more and 0.2 times more compared to the paper filter and the red foam filter, after one minute of the start of the process. For the dust collected on untarred road, the engine speed was 0.3 times more and 0.4 times more compared to the paper filter and the red foam filter respectively. These results show that as the filter gets blocked with time, the air used for combustion reduces in volume as well as the engine speed. To what extent the air quantity or the engine speed reduces depends on the filter type and the dust loading rate, as indicated by the results obtained.

Each graph contains two legendary lines representing the dust collected on the roof top and dust collected on the untarred road. The relationship between the pressure drop and the engine speed at different dust loading rates (0.08 g/s and 0.14 g/s) for the filters are shown in Figures 4.4 (a),

(b) and (c). As shown in the figures, the pressure drop across the filters increase with engine speed within seconds after the start of the process. However, the engine speed reduces with increase in pressure drop just after some time.

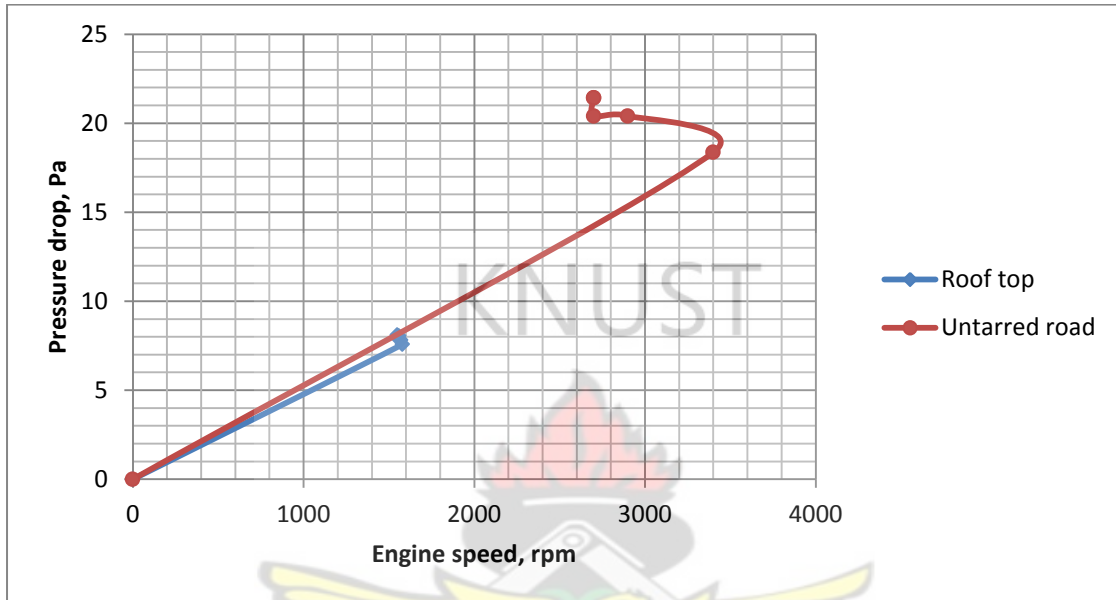


Figure 4.4 (a): Relation between pressure drop and engine speed for the yellow foam filter.



Figure 4.4 (b): Relation between pressure drop and engine speed for the paper filter.

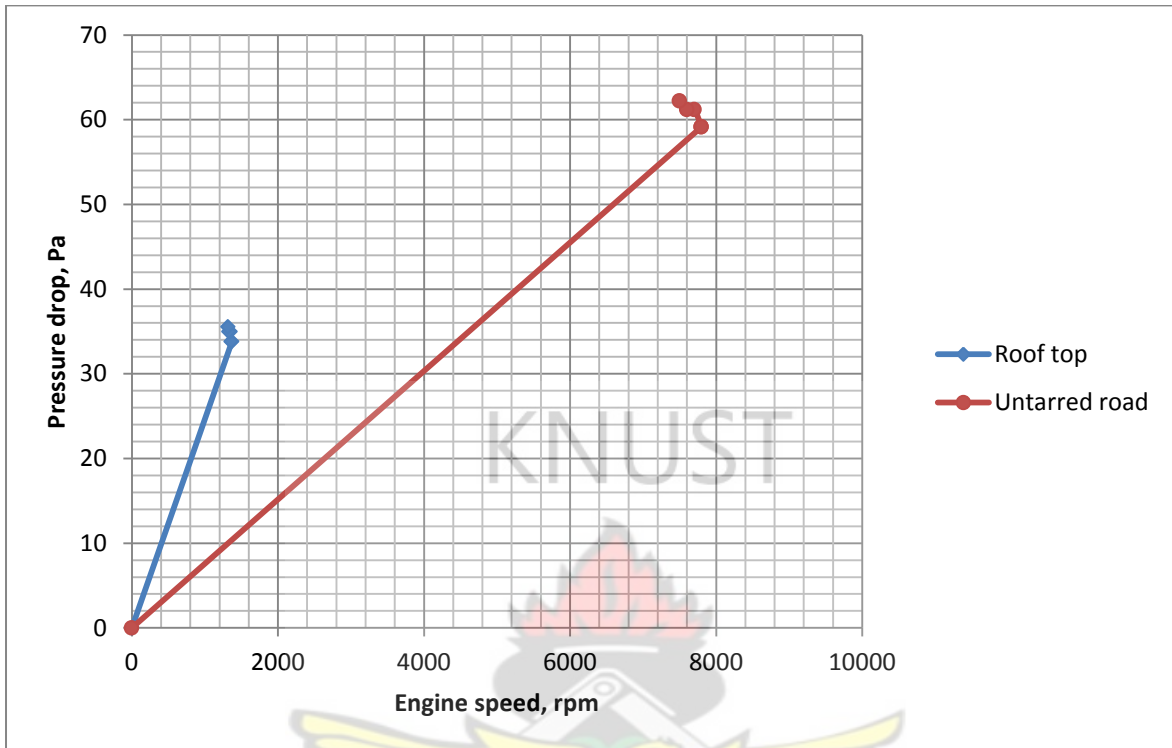


Figure 4.4 (c): Relation between pressure drop and engine speed for the red foam filter.

4.2 Discussion

4.2.1 Effect of dust load on pressure drop across the air filters

The experimental results indicate that the resistance to air flow for all three filters increased sharply at the start of the process to a peak value, dropped slightly and then increased steadily with time. The sharp increase in pressure drop within the first minute is an indication that the pores of the nearest fibres get blocked fast thereby increasing the resistance to air flow through those air passages. The slight decrease in value shows that more pores that had not yet been blocked were exposed along the length of the filter. With time the resistance to air flow increased slightly because most pores got blocked. These results are so to be expected because as air passes

through the filter media, the filter structure causes a resistance that is a measure of air permeability or the pressure drop.

Results of the experiment for foam filter 1 (thickness of 0.1 cm) show that the pressure drop is directly proportional to the dust loading rate. As the dust loading rate increased from 0.08 g/s to 0.14 g/s, it was found that the pressure drop increased about 2.4 times (from 7.6 Pa for 0.08 g/s to 18.4 Pa for 0.14 g/s) within one minute after the start of the process. These results are expected because as more dust enters the filter, the combined effect of each fiber resisting the flow of air past it increases, thereby reducing the amount of air entering the inlet of the engine for combustion. The values obtained also indicated that the pressure drop only increased slightly after some time. This means within the time interval, the amount of air passages blocked by the dust was the same or slightly larger. The values obtained show that the pressure drop will continue to grow indicating clogging of the filter.

The Harmattan dust concentrations are seen to be about two to three orders of magnitude higher than the non-Harmattan aerosol at all particle diameters (Sunnu, et al 2006). This means there are high levels of atmospheric dust pollution during the Harmattan season. Since results of the experiment show that as the dust rate increases, there is an increase in pressure drop with time, this implies that the pressure drop across filters during the Harmattan season will be significantly higher and that it will take less time for the filters to get blocked.

The pressure drop across the filters was also found to increase with engine speed within seconds after the start of the process. This is because within this period, more air passes across the length of the filter and enters the engine as resistance to air flow by the filters has not yet been prominent. However, the engine speed reduces with increase in pressure drop just after some

time. This is expected because with time the air passage ways get blocked with dust particles increasing the resistance to air flow by the filters and thus reducing the amount of air entering the engine for combustion.

4.2.2 Effect of dust load on engine speed and fuel level

The relation between pressure drop and engine speed become steeper with higher dust loading rates. This indicates that the engine runs at relatively low speeds for higher dust loading rates. The fuel level was also recorded and for the 0.08 g/s dust loading, the fuel level drops for foam filter 1 (thickness of 0.1 cm) was 0.6 mm, for the paper filter (thickness of 0.1 cm) it was 0.05 mm and for foam filter 3 (thickness of 0.15 cm) it was 0.03 mm. These results also clearly indicate that a filter with a high fiber thickness and small pore sizes with greater number of fibres does not cause an appreciable decrease in fuel level.

The restrictions imposed by the filter element also will create friction which causes inlet throttling losses. Energy has to be supplied to the piston to produce a pressure difference across the inlet valve so that fresh charge could be drawn into the cylinder. This energy supplied to the piston is an intake stroke loss. Following this argument, a filter structure that produces a low pressure drop is a desirable one. Engine friction will increase with the increase in engine speed, a factor that increases engine friction. The average engine speeds for filters 1, 2 and 3 for the 0.08 g/s dust loading rate are 1600 rpm, 1200 rpm and 1300 rpm. Values for the 0.14 g/s rate are 300 rpm, 700 rpm and 800 rpm. Comparing these values show that as the dust rate increases, the engine speed reduces.

Clearly, in the Harmattan season, the engine will now be running at lower speeds. The implication being that more dust particles will enter the engine and cause mechanical wear of the

moving parts particularly in the piston-cylinder compartment. This can create more clearance which can lead to vibrations being set-up.

4.2.3 Effect of dust load on air flow after the filters

As to be expected, the quantity of air entering the engine after filtration was also found out to be proportional to the pressure drop across the filter within one minute and inversely proportional to the pressure drop after a peak value some seconds after one minute. The results obtained for the three filters show that within one minute, the air flow increases sharply to a peak value some seconds after one minute. The rising increase in air flow during the few seconds indicates that the air passages were not blocked and that the dust particles were not attaching themselves to the filter material. This continued to a peak value that is an indication that dust particles have begun attaching themselves to the filter material. There is a sharp decrease between the peak and some seconds to two minutes indicating that more particles were still attaching themselves and blocking the air passages.

There is now a gradual decrease in air flow just after two minutes; this clearly indicates that most particles might have now attached themselves to the filter material and blocked most air passages. The times it took for filters 1, 2 and 3 to reach their peak were 72 seconds, 74 seconds and 84 seconds respectively for the two dust loading rates but at different peak values. These values also indicate that with the Harmattan season, the time it will take a filter to reach the peak value will approximately be the same but it will take less time (two to three times less) for the filter to get clogged as compared to the non-Harmattan period.

The values obtained give indication that the time it takes for a filter material to get blocked depends on filter material and area occupied by the fibers on the filter. The greater the fiber area of the filter the more time it takes for the filter material to have its air packages blocked.

The dust arrestance/collection efficiency of the filters was also computed (appendix I) and it was found that, the values depend on mass flow rate of dust and fiber thickness. The reason for measuring this parameter was to know how much of dust particles that were arrested by the filters (due to adhesion) and did not penetrate through them.

4.2.4 Kilometer-run of vehicles

The life of air filters fixed on the road vehicle engine is determined by the distance (kilometer) run irrespective of the dustiness/ cleanliness of the ambient air. The air filter manufacturer declares the distance to be covered after which the air filter is changed. For example, the distance declared on the paper filter is as follows, “Change filter every 48 280 km for non-dusty periods”. In this study non- dusty road can be referred to as the tarred road during the non-Harmattan period. The distance run by the vehicle on non-tarred road is not specified and therefore, unknown. The analysis in this section leads to finding the distance run on a dusty, non-tarred road and on tarred road during the Harmattan period.

The mass concentration for the non-dusty period is about $26.67 \mu\text{g}/\text{m}^3$. The mass concentration for the Harmattan period is between 168 and $1331 \mu\text{g}/\text{m}^3$.

$$\text{If } 26.67 \mu\text{g}/\text{m}^3 = 48280 \text{ km}$$

$$\text{then } 168 \mu\text{g}/\text{m}^3 = \frac{26.67}{168} \times 48280 = 7664.45 \text{ km}$$

Also

$$\text{If } 26.67 \mu\text{g}/\text{m}^3 = 48280 \text{ km}$$

$$\text{then } 1331\mu\text{g}/\text{m}^3 = \frac{26.67}{1331} \times 48280 = 967 \text{ km}$$

It is seen from the above calculations that vehicles will cover less kilometer-run for filters to get blocked during the Harmattan season. For example, a vehicle that plies on paved roads in the non-Harmattan season and covers 48 280 km (provided by manufacturer) for its filter to get clogged can only cover between 967 km and 7664 km during the Harmattan period (depending on the mass concentration of the Harmattan period) for the filter to get clogged.



CHAPTER FIVE

CONCLUSION AND RECOMMENDATIONS

This chapter presents the summary of the work, concluding remarks and the recommendations for further work.

5.1 Conclusion

The main objective of this research was to investigate the effect of harmattan dust on air filters in relation to engine performance of vehicles.

It was found that different filters because of structure and shape affect engine performance and effectiveness. Similar trends in engine performance were obtained for the filters tested. However, results show that while some filters (foam filters of longer length with smaller pore sizes) have little effect on engine performance, others (paper filters of shorter length and smaller pore sizes) strongly affected engine performance.

It was also found that dust particles accumulated near the downstream side of the filter. High concentration of particles located at the downstream part is explained by the fact that, besides the particles collected in this area, the dust washed from the upstream part of the filter also passes through the downstream part. This shows that filters get clogged first downstream and gradually moves upstream of the filter.

It has also been seen that when the Harmattan season set in, the pressure drop across filters will increase significantly and cause clogging of the filters within a short period. Air filters in vehicles that ply on untarred roads exhibit higher pressure drops than those used in vehicles on tarred roads.

Air flow measurements also indicated that for filters used on untarred roads, the air flow values are less compared to filters used on paved roads. These values also indicate that it takes a shorter time for filters used on untarred roads to get clogged compared to those used on paved roads.

Analysis also indicated that engine friction will increase significantly during the Harmattan season. This will definitely cause mechanical wear of the moving parts and set up engine vibrations.

It is also seen that vehicles will cover lesser kilometer-run for filters to get blocked during the Harmattan season. For example, a vehicle that plies on paved roads in the non-Harmattan season and covers 48 280 km (provided by manufacturer) for its filter to get clogged can only cover between 967 km and 7664 km during the Harmattan period (depending on the number concentration of the Harmattan period) for the filter to get clogged

It is estimated that the extreme north of the country is under the influence of the Saharan dust aerosol 80% of the time, compared with only 45% for the city of Kumasi and a tiny 8% for the capital city of Accra (Sunnun et al, 2000). This clearly indicates that the effectiveness of filters in relation to engine performance of vehicles used in the north will get more affected based on the analysis made in the discussion than filters used in vehicles in Kumasi and Accra.

5.2 Recommendations

The main recommendations from this thesis are as follows;

- (a) Some vehicles have no means of checking for clogging of filters. Inlet manifolds of engines should be equipped with air flow sensors to indicate when it is appropriate to clean or change

air filters. Air flow measurements provide information on performance of filters in terms of blockage by dust particles.

- (b) Filter materials should be designed to have little affinity for attachment of particles of Harmattan dust or water droplets in case humid air enters the vehicle with dust particles. Filter effectiveness and consequently engine performance is affected only when particles attach themselves to the filter. Filter materials should have less attraction for dust particles to prolong engine performance of vehicles.
- (c) Filters should be changed or regenerated based on air flow measurements but not necessarily by distance covered by vehicles. If filters are changed based on distance covered by vehicles, engine performance will be affected negatively in the case when the filter gets clogged before meeting the distance provided by the manufacturer. Moreover, if the vehicle is used more often on less dusty road, the possibility of the filter getting clogged earlier than the distance required for changing or regeneration is low. Engine performance may not have been affected significantly. Air flow measurements show precisely when to change the filter.
- (d) Harmattan dust data should be used to predict the performance and improvement of other engineering devices, systems and equipment, e.g. solar panel.

REFERENCES

1. Afeti G. M. and F.J Resch (2000). Physical characteristics of Saharan dust near the Gulf of Guinea, *Atmos. Environ.*, 34, 1273-1279.
2. Agarwal J. K. and G. J. Sem (1980). Continuous flow, single-particle-counting condensation nucleus counter, *J. Aerosol Sci.* 11:343 – 57.
3. Allen T. (1968). *Particle Size Measurement*, Chapman and Hall, London.
4. Allen T. (1981). *Particle Size Measurement*, 3rd edition, Methuen, New York.
5. Barth H.G.(ed.). (1984). *Modern Methods of Particle Size Analysis*, Wiley, New York.
6. Beddow J. K. (1980). *Testing and Characterization of Powders and Fine Particles*, Wiley, New York.
7. Beddow J. K. (1984). *Particle Characterization in Technology*, Boca Raton, CRC Press, FL.
8. Bird B. R., Stewart W. E. and E. N. Lightfoot (1960). *Transport Phenomena*, Wiley, New York.
9. Brown R. C. (1993). *Air Filtration – an integrated approach to the theory and applications of fibrous filters*, Pergamon, Oxford.
10. Cadle R. D. (1975). *The Measurement of Airborne Particles*, Wiley, New York, 1975.
11. Cadle, R. D. (1965). *Particle Size – Theory and Industrial Applications*, Van Nostrand Reinhold, New York.
12. Chang Y. S., Yeh H. C. and K.J. Brinsko (1985). *J., Aerosol Sci. Tech.*, 4, 165 – 174.
13. Cheng Y. S. (1988). *Dynamic Shape Factor of Plate-Like Particles*, *Aerosol Sci. Tech.*, 8, 109 – 123.

14. Clayton P. (1981). The Filtration Efficiency of a Range of Filter Media for Submicrometer Aerosols, State Mutual Book, New York.
15. Coutant R. W. (1977). Effect of environmental variables on collection of atmospheric sulfate, Environ. Sci. Technol. 11:873.
16. Davies C. N. (1966). Aerosol Science, Academic Press, New York.
17. Davies C. N. (1973). Air Filtration, Academic Press, London.
18. Davies, C. N. (1979). Coagulation of Aerosols by Brownian Motion, J. Aerosol Sci., 10, 151 – 161.
19. Dorman R. G. (1974). Dust Control and Air Cleaning, Pergamon Press, New York.
20. Friedlander S. K. (1977). Smoke, Dust and Haze, Wiley, New York.
21. Fuchs N. A. (1964). The Mechanics of Aerosols, Pergamon, Oxford.
22. Herdan G. (1953). Small Particle Statistics, Elsevier, New York.
23. Lippman M. and S. Hering (1995). Air Sampling Instruments, 8th edition, Ch. 7, ACGIH, Cincinnati.
24. Lodge J. P., Jr. and T.L Chan (ed.). (1986). Cascade Impactor, Sampling and Data Analysis, Akron, OH.
25. Malissa H. (ed.). (1978). Analysis of Airborne Particles by Physical Methods, Boca Raton, CRC Press, FL.
26. Mednikov E. P. (1965). Acoustic Coagulation and Precipitation of Aerosols, Consultants Bureau, New York.
27. Mercer T. T. (1973). Aerosol Technology in Hazard Evaluation, Academic Press, New York.

28. Ogawa A. (1984). Separation of Particles from Air and Gases, Vols.I and II, Boca Raton, CRC Press, FL.
29. Orr C. and J.M. Dallavalle (1959). Fine Particle Measurement, Macmillan, New York.
30. Rahjans G. S and J. Sullivan (1981). Asbestos Sampling and Analysis, Ann Arbor, MI.
31. Reist P. C. (1993). Introduction to Aerosol Science, McGraw-Hill, New York.
32. Seinfeld J. H. and S.N. Pandis (1998). Atmospheric Chemistry and Physics, Wiley, New York.
33. Silverman L., C. Billings and M. First (1971). Particle Size Analysis in Industrial Hygiene, Academic Press, New York.
34. Sunnu A. K. (2006). An experimental study of the Saharan dust physical characteristics and fluxes near the Gulf of Guinea, PhD Thesis, Universite du Sud Toulon-Var, France.
35. Tien C. (1989). Granular Filtration of Aerosols and Hydrosols, Butterworth, Boston.
36. Vincent J. H. (1989). Aerosol Sampling – science and practice, Wiley, New York.
37. Vincent J. H. (1995). Aerosol Science for Industrial Hygienists, Pergamon, Oxford, UK.
38. White H. J. (1963). Industrial Electrostatic Precipitation, Reading, Addison-Wesley, MA.
39. Willeke K. and P.A Baron (1993). Aerosol measurement - principles, techniques and applications, John Wiley and Sons Inc. New York.
40. Wilson R. and J. Spengler (1996). Particles in our air – concentrations and air effects, Harvard University Press.
41. Zebel G., “Coagulation of Aerosols,” in Davies C. N. (1996). Aerosol Science, Academic Press, New York.

APPENDIX I

MASS FLOW RATES OF DUST AND COLLECTION EFFICIENCY OF FILTERS

1a) Foam filter (yellow)

Mass of container (before) = 0.125 kg

Mass of container + dust (before) = 0.664 kg

∴ Mass of dust (before) = 0.664 – 0.125 = 0.529 kg = 529 g

Mass of filter = 158 g

Mass of filter + dust = 160 g

∴ Mass of dust retained by filter = 160 – 158 = 2 g

Mass of container (after) = 0.64 kg

∴ Mass of dust entering filter = 0.664 – 0.64 = 0.024 kg = 24 g

Mass of dust entering engine inlet = 24 – 2 = 22 g

$$\Rightarrow \text{Mass flow rate of dust} = \frac{\text{mass entering filter}}{\text{time interval}} = \frac{24}{5 \times 60} = 0.08 \text{ g/s}$$

$$\text{Collection efficiency} = \frac{\text{mass of dust retained}}{\text{mass of dust entering filter}} = \frac{2}{24} \times 100 = \mathbf{8.33\%}$$

$$\% \text{ penetration} = \frac{\text{mass of dust entering engine inlet}}{\text{mass of dust entering filter}} = \frac{22}{24} \times 100 = 91.7\%$$

1b) Foam filter (yellow)

Mass of container (before) = 0.125 kg

Mass of container + dust (before) = 0.925 kg

∴ Mass of dust (before) = 0.925 – 0.125 = 0.8 kg = 800 g

Mass of filter = 158 g

Mass of filter + dust = 161 g

∴ Mass of dust retained by filter = 161 – 158 = 3.0 g

Mass of container (after) = 0.883 kg

∴ Mass of dust entering filter = 0.925 – 0.883 = 0.042 kg = 42 g

Mass of dust entering engine inlet = 42 – 3 = 39 g

$$\Rightarrow \text{Mass flow rate of dust} = \frac{\text{mass entering filter}}{\text{time interval}} = \frac{42}{5 \times 60} = 0.14 \text{ g/s}$$

$$\text{Collection efficiency} = \frac{\text{mass of dust retained}}{\text{mass of dust entering filter}} = \frac{3}{42} \times 100 = 7.14\%$$

$$\% \text{ penetration} = \frac{\text{mass of dust entering engine inlet}}{\text{mass of dust entering filter}} = \frac{39}{42} \times 100 = 92.9\%$$

2a) Paper filter (red)

Mass of container (before) = 0.145 kg

Mass of container + dust (before) = 0.674 kg

∴ Mass of dust (before) = 0.674 – 0.145 = 0.529 kg = 529 g

Mass of filter = 195 g

Mass of filter + dust = 198.6 g

∴ Mass of dust retained by filter = 198.6 – 195 = 3.6 g

Mass of container (after) = 0.65 kg

∴ Mass of dust entering filter = 0.674 – 0.65 = 0.024 kg = 24 g

Mass of dust entering engine inlet = 24 – 3.6 = 20.4 g

$$\Rightarrow \text{Massflowrateof dust} = \frac{\text{massenteringfilter}}{\text{timeinterval}} = \frac{24}{5 \times 60} = 0.8 \text{ g/s}$$

$$\text{Collectionefficiency} = \frac{\text{massofdustretained}}{\text{massofdustenteringfilter}} = \frac{3.6}{24} \times 100 = 15\%$$

$$\% \text{ penetration} = \frac{\text{massofdustenteringengineinlet}}{\text{massofdustenteringfilter}} = \frac{20.4}{24} \times 100 = 85\%$$

2b) Paper filter (red)

Mass of container (before) = 0.145 kg

Mass of container + dust (before) = 0.945 kg

∴ Mass of dust (before) = 0.945 – 0.145 = 0.8 kg = 800 g

Mass of filter = 195 g

Mass of filter + dust = 200.4 g

∴ Mass of dust retained by filter = 200.4 – 195 = 5.4 g

Mass of container (after) = 0.903 kg

∴ Mass of dust entering filter = 0.879 – 0.837 = 0.042 kg = 42 g

Mass of dust entering engine inlet = 42 – 5.4 = 36.6 g

$$\Rightarrow \text{Massflowrateof dust} = \frac{\text{massenteringfilter}}{\text{timeinterval}} = \frac{42}{5 \times 60} = 0.14 \text{ g/s}$$

$$\text{Collection efficiency} = \frac{\text{mass of dust retained}}{\text{mass of dust entering filter}} = \frac{5.4}{42} \times 100 = 12.9\%$$

$$\% \text{ penetration} = \frac{\text{mass of dust entering engine inlet}}{\text{mass of dust entering filter}} = \frac{36.6}{42} \times 100 = 87.1\%$$

3a) Foam filter (red)

Mass of container (before) = 0.128 kg

Mass of container + dust (before) = 0.657 kg

∴ Mass of dust (before) = 0.657 – 0.128 = 0.529 kg = 529 g

Mass of filter = 300 g

Mass of filter + dust = 306.5 g

∴ Mass of dust retained by filter = 306.5 – 300 = 6.5 g

Mass of container (after) = 0.633 kg

∴ Mass of dust entering filter = 0.657 – 0.633 = 0.024 kg = 24 g

Mass of dust entering engine inlet = 24 – 6.5 = 17.5 g

$$\Rightarrow \text{Mass flow rate of dust} = \frac{\text{mass entering filter}}{\text{time interval}} = \frac{24}{5 \times 60} = 0.08 \text{ g/s}$$

$$\text{Collection efficiency} = \frac{\text{mass of dust retained}}{\text{mass of dust entering filter}} = \frac{6.5}{24} \times 100 = 27.1\%$$

$$\% \text{ penetration} = \frac{\text{mass of dust entering engine inlet}}{\text{mass of dust entering filter}} = \frac{17.5}{24} \times 100 = 72.9\%$$

3b) Foam filter (red)

Mass of container (before) = 0.128 kg

Mass of container + dust (before) = 0.928 kg

∴ Mass of dust (before) = 0.928 – 0.128 = 0.8 kg = 800 g

Mass of filter = 300 g

Mass of filter + dust = 309.8 g

∴ Mass of dust retained by filter = 306.5 – 300 = 9.8 g

Mass of container (after) = 0.886 kg

∴ Mass of dust entering filter = 0.928 – 0.886 = 0.042 kg = 42 g

Mass of dust entering engine inlet = 42 – 9.8 = 32.2 g

$$\Rightarrow \text{Mass flow rate of dust} = \frac{\text{mass entering filter}}{\text{time interval}} = \frac{42}{5 \times 60} = 0.14 \text{ g/s}$$

$$\text{Collection efficiency} = \frac{\text{mass of dust retained}}{\text{mass of dust entering filter}} = \frac{9.8}{42} \times 100 = 23.3\%$$

$$\% \text{ penetration} = \frac{\text{mass of dust entering engine inlet}}{\text{mass of dust entering filter}} = \frac{32.2}{42} \times 100 = 76.7\%$$

APPENDIX II

SOLIDITY/PACKING DENSITY OF THE FILTERS

1) FOAM FILTER 1

$$\text{Total volume} = 15 \times 20.3 \times 3.8 = 1157.1 \text{ cm}^3$$

$$\text{Volume occupied by one fibre} = 2.3 \times 0.1 \times 13.8 = 3.174 \text{ cm}^3$$

$$\therefore \text{Total fibre volume} = 3.174 \times 58 = 184.09 \text{ cm}^3$$

$$\text{Solidity, } \alpha = \frac{\text{fibre volume}}{\text{total volume}} = \frac{184.09}{1157.1} = \mathbf{0.16}$$

2) PAPER FILTER 2

$$\text{Total volume} = 16.5 \times 27.7 \times 3.5 = 1599.7 \text{ cm}^3$$

$$\text{Volume occupied by one fibre} = 1.6 \times 0.1 \times 14.5 = 2.32 \text{ cm}^3$$

$$\therefore \text{Total fibre volume} = 2.32 \times 62 = 143.84 \text{ cm}^3$$

$$\text{Solidity, } \alpha = \frac{\text{fibre volume}}{\text{total volume}} = \frac{143.84}{1599.7} = \mathbf{0.09}$$

3) FOAM FILTER 3

$$\text{Total volume} = 16.9 \times 27.9 \times 3.5 = 1650.3 \text{ cm}^3$$

$$\text{Volume occupied by one fibre} = 1.6 \times 0.15 \times 14.5 = 3.48 \text{ cm}^3$$

$$\therefore \text{Total fibre volume} = 3.48 \times 52 = 180.96 \text{ cm}^3$$

$$\text{Solidity, } \alpha = \frac{\text{fibre volume}}{\text{total volume}} = \frac{180.96}{1650.3} = \mathbf{0.11}$$